Neurobiology of Disease

NOX1/NADPH Oxidase Promotes Synaptic Facilitation Induced by Repeated D_2 Receptor Stimulation: Involvement in Behavioral Repetition

Nozomi Asaoka,[1] Masakazu Ibi,[1] Hikari Hatakama,[2] Koki Nagaoka,[2] Kazumi Iwata,[1] Misaki Matsumoto,[1] Masato Katsuyama,[3] Shuji Kaneko,[2] and Chihiro Yabe-Nishimura[1]

[1]Department of Pharmacology, Kyoto Prefectural University of Medicine, Kyoto, 602-8566, Japan, [2]Department of Molecular Pharmacology, Graduate School of Pharmaceutical Sciences, Kyoto University, Kyoto, 606-8501, Japan, and [3]Radioisotope Center, Kyoto Prefectural University of Medicine, Kyoto, 602-8566, Japan

Repetitive behavior is a widely observed neuropsychiatric symptom. Abnormal dopaminergic signaling in the striatum is one of the factors associated with behavioral repetition; however, the molecular mechanisms underlying the induction of repetitive behavior remain unclear. Here, we demonstrated that the NOX1 isoform of the superoxide-producing enzyme NADPH oxidase regulated repetitive behavior in mice by facilitating excitatory synaptic inputs in the central striatum (CS). In male C57Bl/6J mice, repeated stimulation of D_2 receptors induced abnormal behavioral repetition and perseverative behavior. *Nox1* deficiency or acute pharmacological inhibition of NOX1 significantly shortened repeated D_2 receptor stimulation-induced repetitive behavior without affecting motor responses to a single D_2 receptor stimulation. Among brain regions, *Nox1* showed enriched expression in the striatum, and repeated dopamine D_2 receptor stimulation further increased *Nox1* expression levels in the CS, but not in the dorsal striatum. Electrophysiological analyses revealed that repeated D_2 receptor stimulation facilitated excitatory inputs in the CS indirect pathway medium spiny neurons (iMSNs), and this effect was suppressed by the genetic deletion or pharmacological inhibition of NOX1. *Nox1* deficiency potentiated protein tyrosine phosphatase activity and attenuated the accumulation of activated Src kinase, which is required for the synaptic potentiation in CS iMSNs. Inhibition of NOX1 or β-arrestin in the CS was sufficient to ameliorate repetitive behavior. Striatal-specific *Nox1* knockdown also ameliorated repetitive and perseverative behavior. Collectively, these results indicate that NOX1 acts as an enhancer of synaptic facilitation in CS iMSNs and plays a key role in the molecular link between abnormal dopamine signaling and behavioral repetition and perseveration.

Key words: behavioral repetition; dopamine; NADPH oxidase; obsessive-compulsive disorder; striatum

Significance Statement

Behavioral repetition is a form of compulsivity, which is one of the core symptoms of psychiatric disorders, such as obsessive-compulsive disorder. Perseveration is also a hallmark of such disorders. Both clinical and animal studies suggest important roles of abnormal dopaminergic signaling and striatal hyperactivity in compulsivity; however, the precise molecular link between them remains unclear. Here, we demonstrated the contribution of NOX1 to behavioral repetition induced by repeated stimulation of D_2 receptors. Repeated stimulation of D_2 receptors upregulated *Nox1* mRNA in a striatal subregion-specific manner. The upregulated NOX1 promoted striatal synaptic facilitation in iMSNs by enhancing phosphorylation signaling. These results provide a novel mechanism for D_2 receptor-mediated excitatory synaptic facilitation and indicate the therapeutic potential of NOX1 inhibition in compulsivity.

Received Aug. 12, 2020; revised Jan. 21, 2021; accepted Jan. 27, 2021.

Author contributions: N.A., S.K., and C.Y.-N. designed research; N.A., M.I., H.H., and K.N. performed research; N.A., M.I., and M.K. contributed unpublished reagents/analytic tools; N.A., M.I., H.H., K.N., K.I., M.M., and M.K. analyzed data; N.A. wrote the first draft of the paper; N.A., S.K., and C.Y.-N. edited the paper; N.A. wrote the paper.

C.Y.-N. is the cofounder of a startup company developing NOX inhibitors. The remaining authors declare no competing financial interests.

This work was supported in part by Japanese Society for the Promotion of Science Grants-in-Aid for Scientific Research, Uehara Memorial Foundation, and Suzuken Memorial Foundation to N.A. We thank Dr. Takayuki Nakagawa and Dr. Hisashi Shirakawa for intellectual advice and comments on the manuscript.

Correspondence should be addressed to Nozomi Asaoka at nasaoka@koto.kpu-m.ac.jp.

https://doi.org/10.1523/JNEUROSCI.2121-20.2021

Introduction

Striatal dopaminergic signaling is3 required for behavior control and the disruption of this control causes various compulsive/impulsive behaviors (Hyman and Malenka, 2001; Tritsch and Sabatini, 2012). Compulsive repetition of a single or sequence of behaviors is one of the core symptoms of psychiatric disorders, such as obsessive-compulsive behavior (OCD) (Robbins et al., 2019). A similar stereotypy, called punding, is observed in dopaminergic agent users, such as patients with Parkinson's disease and psychostimulant abusers (Voon et al., 2009; Fasano and

Petrovic, 2010). The findings of clinical and animal studies both suggest that long-term (repeated) use and/or a high dose of dopaminergic agents contribute to the prevalence of stereotypy (Szechtman et al., 1998; Vanderschuren and Everitt, 2004; Fasano and Petrovic, 2010), suggesting the involvement of sustained neuroadaptation to dopaminergic agents (e.g., sensitization) (Bailey et al., 2008). In line with this hypothesis, we have previously demonstrated that repeated stimulation of dopamine D_2 receptors elicited compulsive behaviors, including spontaneous repetitive behavior (Asaoka et al., 2019). However, the molecular mechanisms underlying the repetitive behavior induced by repeated stimulation of dopamine receptor(s) remain unclear.

Cortical information received by the striatum is differentially processed by two types of medium spiny neurons (MSNs). The balance between the activity of D_1 receptor-expressing direct pathway MSNs (dMSNs) and D_2 receptor-expressing indirect pathway MSNs (iMSNs) contributes to action control (Bariselli et al., 2019), and disruption of this balance is suggested to cause compulsivity (Bock et al., 2013; Wang et al., 2017). Since changes in the binding potential of striatal D_2 receptors have been reported in psychiatric disorders with compulsivity (e.g., OCD [Denys et al., 2004], Parkinson's disease [Farkas et al., 2012], and addiction [Fehr et al., 2008]), altered dopaminergic signaling toward iMSNs may be a key pathologic mechanism for compulsive repetitive behavior. In support of this idea, antipsychotics with antagonist activity at D_2 receptors are widely used in augmentation therapy for OCD (Bloch et al., 2006), suggesting the involvement of striatal D_2 receptors in both pathophysiological and therapeutic mechanisms for compulsivity.

Low concentrations of reactive oxygen species (ROS) modify the function of multiple proteins largely through the oxidation of cysteine residues (Holmström and Finkel, 2014). NADPH oxidase (NOX), which catalyzes electron transfer from NADPH to molecular oxygen, is one of the sources of ROS in the CNS (Sorce et al., 2012). Among NOX subtypes, NOX1, NOX2, and NOX4 are mainly expressed in the brain (Sorce et al., 2012). Although the phagocyte oxidase NOX2 has been extensively examined, particularly in the field of neuroinflammation, the physiological and pathologic roles of nonphagocytic NOXs in the CNS are still being investigated. We recently reported that nonphagocytic NOX1 regulated depression-like behavior in mice (Ibi et al., 2011), suggesting the involvement of NOX1 in neuropsychiatric disorders.

In the present study, we examined the involvement of NOX1 in compulsive behavioral repetition using the repeated D_2 receptor stimulation protocol. Behavioral abnormalities induced by sensitization to a D_2 receptor agonist, quinpirole (QNP), were assessed in *Nox1*-deficient mice. Sensitization-induced synaptic and molecular changes were investigated both *in vivo* and *in vitro*. The present results demonstrated the novel function of NOX1 in inducing a shift in D_2 receptor signaling from inhibition to facilitation of central striatum (CS) iMSNs, which may lead to compulsive behavioral repetition.

Materials and Methods

Animals. All procedures were conducted in accordance with the ethical guidelines of the Animal Research Committee of the Kyoto Prefectural University of Medicine. Male C57BL/6J mice (RRID:IMSR_JAX:000664) were purchased from Nihon SLC. *Nox1* KO mice ($Nox1^{-/Y}$) on a C57BL/6J background were maintained in our laboratory (Matsuno et al., 2005). WT littermates for *Nox1* KO mice were used for the "WT versus KO" experiments. Mice (6-24 weeks old) were housed at a constant ambient temperature of 24 ± 1°C on a 12 h light-dark cycle with access to food and water *ad libitum*.

For sensitization to D_2 receptor stimulation, mice were intraperitoneally injected with QNP (1 mg/kg) every weekday. Mice that received 7-12 injections of QNP were used in the sensitized (Sens) group (Asaoka et al., 2019).

Reagents. (−)-QNP, a dopamine D_2 agonist (Tocris Bioscience), was dissolved in water or saline. Bicuculline (a $GABA_A$ antagonist; Enzo Life Science), ML171 (a NOX1 inhibitor; Tokyo Chemical), UNC9994 (an arrestin-biased D_2 agonist; Axon MedChem), Barbadin (a β-arrestin inhibitor; Axon MedChem), PP2 (an Src kinase inhibitor; Abcam Biochemicals), and setanaxib (a NOX1/4 inhibitor; Axon MedChem) were dissolved in DMSO. Stock solutions were stored at −20°C until use and dissolved in saline, 1%-5% Tween 80 solution, ACSF, or pipette solution. The final concentration of DMSO was <5% for intraperitoneal injection and microinjection, 0.05% for electrophysiology.

Recording of repetitive behavior. Mice were singly housed, and spontaneous behavior in their home cage was recorded for 10 min. Recording was started 20 min after the last drug injection, when the chewing is most strongly induced (Asaoka et al., 2019). The types of assessed behaviors were as follows: walking, chewing, rearing, leaning, grooming, and digging. The end of the behavioral bout was defined by starting other type of behavior or, in rare cases, freezing >1 s. Repeated chewing behavior consisted of the following sequence of behaviors: holding a wood chip in the forelimbs and gently biting and pulling the chip by the mouth and forelimbs. Movement of the head and/or forelimbs toward their own fur (grooming) or to push wood chips (digging) was separately counted. Time spent for each behavior was counted manually. The assessor was blinded to treatment condition assignment.

In our pervious study, we showed that 8 time injections maximize the time spent chewing, which was stable during, at least, 8-12 injections (Asaoka et al., 2019). Based on this observation, mice receiving 8 or 9 injections of QNP were used as the sensitized group. The number of injections was counterbalanced between groups. To acutely inhibit NOX1, ML171 (50 mg/kg, i.p.) was injected 5 min before the last injection of QNP.

Open field test. One day before the experiment (day 0), mice were allowed to explore an open field (75 × 75 cm) for 10 min. To examine the effect of single injection of QNP, mice were placed at the center of the same open field chamber immediately after injection of QNP or saline and locomotor activity was monitored for 30 min on day 1. On day 2, mice received another treatment before open field test. To examine the effect of local infusion of inhibitors, mice received intra-CS infusion of vehicle, barbadin or setanaxib (see Stereotaxic surgery and microinjection) and locomotor activity was monitored for 30 min. Tests were performed 3 consecutive days. The order of treatment was counterbalanced. The total distance traveled during the last 10 min of recording period was analyzed using a video tracking system (ANY-maze version 4.99).

Spatial discrimination learning and reversal learning. The spatial discrimination task was performed as previously described (Asaoka et al., 2019). Briefly, mice were food-restricted (2-3 g/d) on weekdays (80%-90% of the *ad libitum* body weight). After habituation to the T-maze apparatus, mice received a 3-step task as follows; 6 or 7 d training (5 trials/day), 8 d overtraining (5 trials/day), and 4 d reversal learning (10 trials/d). The rewarded goal arm (rewarded with 100 μl of sweetened milk) was randomly chosen and fixed during the training and overtraining periods. For reversal learning, the rewarded arm was reversed, and mice underwent 10 free-choice trials per day for 4 d (R1-R4). For the sensitized group, mice received QNP injection during overtraining and reversal learning phases. To avoid sedative effect, the first two injections were performed after finishing the trials; and from then onwards, mice received injection 20 min before starting the trials. The total number of injections of QNP was 8 at the end of overtraining phase and 12 at the end of reversal learning phase in all group.

Stereotaxic surgery and microinjection. Mice were anesthetized with sodium pentobarbital (50 mg/kg, i.p., Nakarai Tesque) and fixed on a small animal stereotaxic frame (Narishige). For intra-CS injection of inhibitors, guide cannulae were bilaterally implanted directed at the CS (AP 1.2 mm, ML 2.0 mm, DV 3.8 mm from the bregma, angled 10°). On

the experimental day, the drug (1 μg setanaxib or barbadin in 1 μl) was injected through the injection cannula at a rate of 0.15 μl/min. After injection, the injection cannula was left in place for 5 min (for setanaxib) or 10 min (for barbadin). After experiments, 0.5 μl of Evans Blue solution was injected through the cannula to confirm the injection site. When injection site was incorrect, the animal was excluded from analysis.

For striatum-specific silencing of *Nox1*, the adeno-associated virus (AAV) vector expressing miRNA targeting NOX1 or control miRNA was bilaterally injected into the striatum (AP 1.2 mm, ML 1.6 mm, DV 3.9 mm from the bregma). The AAV vectors were prepared as previously described (Ibi et al., 2011), replacing the promoter region with the human synapsin (hSyn) promoter. For spatial discrimination task, habituation to the T-maze apparatus was started after at least 1 week of recovery period, and the overtraining period (combined with repeated injection of QNP) was started 3 or more weeks after the viral infection. For other experiments, mice were used at least 3 weeks after viral infection.

Electrophysiological recordings. Electrophysiological recordings were performed as previously described (Asaoka et al., 2019) with minor modifications.

For acute slice preparation, mice were deeply anesthetized with isoflurane and decapitated. Coronal brain slices (200 μm thick) were prepared with a vibratome (VT1000S, Leica Microsystems) filled with ice-cold cutting solution (composition of the following in mM: 120 NMDG-Cl, 2.5 KCl, 26 $NaHCO_3$, 1.25 NaH_2PO_4, 0.5 $CaCl_2$, 7 $MgCl_2$, 15 D-glucose, and 1.3 ascorbic acid, pH 7.2). Slices were recovered in oxygenated ACSF (composition of the following in mM: 124 NaCl, 3 KCl, 26 $NaHCO_3$, 1 NaH_2PO_4, 2.4 $CaCl_2$, 1.2 $MgCl_2$, and 10 D-glucose, pH 7.3) at 32°C for at least 1 h before recording. After recovery, individual slices were transferred to a recording chamber with continuous perfusion of oxygenated ACSF. ACSF was heated to keep the recording chamber at 27 ± 1°C. Recordings were performed only within 4 h after recovery.

Electrophysiological recordings were performed with an EPC9 amplifier (HEKA), and the data were recorded using Patchmaster software (HEKA). The resistance of the electrodes was 3-7 MΩ when filled with the internal solution (composition of the following in mM: 140 K-gluconate, 5 KCl, 10 HEPES, 2 Na-ATP, 2 $MgCl_2$, and 0.2 EGTA, pH 7.3, adjusted with KOH for current-clamp recordings and 120 $CsMeSO_4$, 15 CsCl, 8 NaCl, 10 HEPES, 2 Mg-ATP, 0.3 Na-GTP, 0.2 EGTA, 10 TEA-Cl, and 5 QX-314, pH 7.3, adjusted with CsOH for EPSC recordings). Individual neurons were visualized with a microscope equipped with a 40× water-immersion objective lens (Carl Zeiss) and a CCD camera. The series resistance was compensated by 70% and maintained within 35 MΩ.

When recording from lateral orbitofrontal cortex (lOFC) pyramidal neurons, neurons showing regular-spiking activity were used for experiments. For recording from MSNs, MSNs were determined by their morphologic features, single-cell RT-PCR was performed for identification of cell types, that is, dMSNs (*Pdyn*-positive) and iMSNs (*Pdyn*-negative and *Penk*-positive) (Asaoka et al., 2019).

For current-clamp recordings, holding current was set at 0 pA. Action potentials were evoked by current injection (0-500 pA, 1 s duration for lOFC and 0.5 s duration for CS).

For recording EPSCs, the membrane potential was held at −70 mV and the $GABA_A$ antagonist (20 μM bicuculline) was continuously perfused. AMPA-mediated evoked EPSCs (eEPSCs) and mixed AMPA- and NMDA-mediated eEPSCs were evoked by stimulation at −70 and 40 mV, respectively. NMDA-mediated eEPSC amplitude was determined as the average amplitude between 45 and 55 ms after stimulation. The average of 5 consecutive AMPA- and NMDA-mediated eEPSC measurements was used for analysis. Drug-induced changes in eEPSC amplitude were calculated by recording before and after the 5 min perfusion of QNP (10 μM) or UNC9994 (10 μM). The concentration of 10 μM was selected according to the previous reports (Li et al., 2011; Xia et al., 2017). AMPAR-mediated eEPSC was normalized by NMDAR-mediated eEPSC. After recording, single-cell RT-PCR was performed to identify cell types, that is, dMSNs (*Pdyn*-positive) and iMSNs (*Pdyn*-negative and *Penk*-positive).

Events were analyzed by Minianalysis software (SynaptoSoft) and Win EDR 3.7.3 (University of Strathclyde).

Preparation of brain tissue samples. Mice were deeply anesthetized with isoflurane and decapitated. Coronal brain slices were prepared with a 1 mm coronal mouse brain slicer. Each brain region was dissected out, using a razor blade, according to a mouse brain atlas (Franklin and Paxinos, 2007). The dorsal striatum (DS) and CS samples were prepared as follows: The striatal region (DS + CS) was dissected from the coronal brain slice (AP ~0.1-1.4 mm from bregma) by removing the area outside of the corpus callosum, anterior commissure, and ventricle. The remaining region was divided in the DS and CS by straight line angled at 10°-20° so that the CS region contains OFC projecting region, which contributes to compulsive repetitive behavior (Ahmari et al., 2013). Dissected samples were stored in RNAlater solution (Sigma Millipore) at 4°C for mRNA isolation. For other experiments, samples were immediately frozen in liquid N_2 and stored at −80°C.

Primary striatal neuronal culture. A primary culture of striatal neurons was prepared from C57BL/6J mice at the embryo stage (E14-E16). Striatal sections were dissociated into single cell suspensions by 0.25% trypsin/1 mM EDTA solution (Nacalai Tesque). Cells were plated on coverslips or culture plates coated with poly-D-lysine (Sigma Millipore) and maintained in Neurobasal Plus medium (Thermo Fisher Scientific) containing 2% B-27 Plus supplement (Thermo Fisher Scientific) and 1% penicillin/streptomycin/glutamine mixed solution (Nacalai Tesque) at 37°C in a humidified atmosphere containing 5% CO_2. Half of the culture medium was replaced with fresh medium every 2-3 d.

After 6-7 d of culture, cells were treated with AAV-hSyn-miR/NOX1 or AAV-hSyn-miR/control and cultured for an additional 7 d for subsequent experiments.

One week after AAV infection, cells were washed with Krebs-Ringer buffer (composition of the following in mM: 140 NaCl, 5 KCl, 1 $MgCl_2$, 2 $CaCl_2$, 10 glucose, and 10 HEPES, pH 7.4) to remove antioxidants in the medium. After washing, cells were preincubated in Krebs-Ringer buffer for 30 min and further incubated with QNP (1 μM) or UNC9994 (1 μM) for 20 min.

In vitro *overexpression of NOX1.* Plasmids for expression of human NOX1 (pCMV-hNOX1), human NOXO1 (pCMV-hNOXO1), and human NOXA1 (pCMV-hNOXA1) were previously constructed (Arakawa et al., 2006). FLAG-tagged human DRD2 (pCMV-FLAG-hDRD2) was obtained from DRD2-TANGO plasmid (Kroeze et al., 2015) (Addgene plasmid #66 269) by using In-Fusion HD Cloning Kit (Takara).

HEK293T cells were cultured in DMEM with GlutaMAX (Thermo Fisher Scientific) supplemented with 10% heat-inactivated FBS (Sigma Millipore) and maintained at 37°C in a humidified incubator set at 5% CO_2. Cells were transfected with pCMV-hNOXO1, pCMV-hNOXA1, pCMV-FLAG-hDRD2, and pCMV-hNOX1 (overexpression group) or pcDNA3.1 (control group). After 36-48 h, cells were incubated in Krebs-Ringer buffer containing drug(s) for 20 min. For immunostaining, transfected cells were replated onto poly-D-lysine-coated glass coverslips and labeled with rabbit anti-DYKDDDDK tag (1:1000, #2368, Cell Signaling Technology) for 1 h at 4°C just before drug treatment.

Real-time qRT-PCR. Real-time qRT-PCR was performed as previously described (Asaoka et al., 2015) with minor modifications. Total mRNA was isolated by NucleoSpin RNA Kit (Toyobo). Samples were diluted to equalize cDNA concentration among samples, and reverse-transcribed by ReverTra Ace qPCR RT Kit (Toyobo). Real-time qRT-PCR was performed using the StepOne real-time PCR system (Invitrogen) with THUNDERBIRD SYBR qPCR Mix (Toyobo). The oligonucleotide primers used were as follows: 5′-CTGACAAGTACTATTACACGAGAG-3′ and 5′-CATATATGCCACCAGCTTATGGAAG-3′ for *Nox1*; 5′-CCCTTTGGTACAGCCAGTGAAGAT-3′ and 5′-CAATCCCGGCTCCCACTAACATCA-3′ for *Nox2*; 5′-GGATCACAGAAGGTCCCTAGCAG-3′ and 5′-GCGGCTACAGCACACCTGAGAA-3′ for *Nox4*; 5′-TGATATGGCGGAGAATGG-3′ and 5′-CTGGTGCTTGACAGCATCTC-3′ for *Drd2*; and 5′-CTTACTCCTTGGAGGCCATGTAG-3′ and 5′-TGTCAAGCTCATTTCCTGGTATGA-3′ for *Gapdh*. Primers for *Nox1* were designed for the sequence deleted in *Nox1* KO mice.

Phosphatase activity assay. Phosphatase activity was quantified by a hydrolysis reaction against p-nitrophenylphosphate (Lorenz, 2011).

Brain tissue or cells were collected in RIPA buffer containing protease inhibitor (Nacarai Tesque). For brain samples, tissue was homogenized by hand-operated homogenizer. The samples were centrifuged at $7000 \times g$ for 10 min, and the supernatants were collected as protein samples. Protein samples were diluted in assay solution (composition of the following in mM: 150 NaCl, 10 Tris-HCl, pH 8.0, 5 $MgCl_2$, 1 EGTA, and 6 p-nitrophenylphosphate) at a ratio of 1:5. After mixing, samples were incubated at 37°C for 2 h and absorbance at 405 nm was measured. The absorbance was normalized by the protein concentration. The activities of protein tyrosine phosphatase (PTP) and protein serine/threonine phosphatase (PP) were evaluated based on differences in absorbance between no inhibitor condition (total activity) and sodium orthovanadate (100 μM; for PTP inhibition) or okadaic acid (100 nM; for PP inhibition).

SDS-PAGE. Brain tissue or cells were collected in RIPA buffer containing protease inhibitor (Nacalai Tesque), 0.1% SDS, and 0.1% phosphatase inhibitor cocktail 2 and 3 (Sigma Millipore). Brain samples were homogenized by hand-operated homogenizer. The samples were centrifuged at $7000 \times g$ for 10 min, and the supernatants were collected. Protein sample were subjected to 10% SDS-PAGE and transferred to a PVDF (Millipore). After blotting, membranes were blocked for 30 min with Blocking-One P (Nacalai Tesque) and incubated for 1 h at room temperature or overnight at 4°C with primary antibodies as follows: rabbit anti-phospho Src family (1:1000, #2101, Cell Signaling Technology), rabbit anti-Src family (1:1000, #2109, Cell Signaling Technology), or mouse anti-β-actin (1:10,000, #A-1978, Sigma Millipore). After washing, the blots were incubated for 1 h at room temperature with HRP-conjugated secondary antibodies. Proteins were visualized by Immobilon Western HRP substrate (Millipore) and detected using Ez-Capture MG (ATTO). Images were analyzed with ImageJ software (National Institutes of Health).

Immunostaining. For primary neuronal culture, cells were fixed with 4% PFA and blocked by 10% horse serum and 0.1% Triton-X containing PBS for 30 min at room temperature. After blocking, cells were incubated primary antibody for MAP2 (rabbit anti-MAP2 antibody, 1:1000; Sigma Millipore) or GFAP (rabbit anti-GFAP antibody, 1:1000; Dako) overnight at 4°C. After washing out the primary antibody, cells were incubated with fluorescence-labeled secondary antibodies (AlexaFluor-conjugated donkey anti-rabbit IgG, 1:1000; Thermo Fisher Scientific) at room temperature for 2 h.

For HEK293T cell, cells were fixed with 4% PFA and blocked by 10% horse serum and 0.1% Triton-X containing PBS for 15 min at room temperature, and were labeled with fluorescence-labeled secondary antibodies (AlexaFluor-conjugated donkey anti-rabbit IgG, 1:500; Thermo Fisher Scientific) and fluorescein-conjugated *Phaseolus vulgaris* leucoagglutinin (PHA-L, 1:500; Vector Laboratories) at room temperature for 2 h.

Fluorescence was visualized using laser scanning confocal microscope (Fluoview FV10i; Olympus). To examine intracellular localization of D_2 receptors, immunofluorescence for FLAG-hDRD2 was analyzed by selecting a straight line across the cell and using the plot profile function of ImageJ software (National Institutes of Health) (Ibi et al., 2008). Intracellular areas were determined by the area between membrane regions identified by PHA-L binding. Average fluorescence intensity of the intracellular region against the total fluorescence intensity across a line bisecting the cell was compared between treatment groups.

Statistical analysis. All data are presented as mean ± SEM. Statistical analyses were performed with GraphPad Prism 5 (GraphPad) and Python (version 3.8.2; http://www.python.org) with the SciPy package (version 1.2.3). Differences with $p < 0.05$ were considered significant. The differences between two groups were compared by a two-tailed Student's *t* test or unpaired *t* test with Welch's correction. When differences within a mouse were compared, a two-tailed paired *t* test was used for analysis. The differences among more than three groups were evaluated by ANOVA with *post hoc* Tukey's multiple comparison test or two-way ANOVA with *post hoc* Bonferroni test. For spatial discrimination task, current injection experiments, and eEPSC recordings, two-way ANOVA for repeated measures and following Bonferroni post-test or three-way ANOVA for repeated measures and following Sidak's multiple comparisons test were used for analysis. Analyses for cumulative probability were performed by a two-sample Anderson–Darling test.

Results

Nox1 deficiency ameliorated compulsive-like behaviors induced by repeated D_2 receptor stimulation

We examined the effects of *Nox1* deficiency on behavioral responses to D_2 receptor stimulation. To investigate whether NOX1 disrupted the D_2 receptor response itself, we examined the sedative effects of a single injection of a D_2 receptor agonist, QNP (1 mg/kg) in *Nox1* KO versus WT mice (Fig. 1*A*). After the single injection, locomotor activity was reduced in both WT and KO mice, and no significant differences were observed between genotypes (Fig. 1*B*,*C*), suggesting that NOX1 deficiency did not affect acute D_2 receptor-mediated locomotion.

Excessive/inappropriate behavioral repetition is considered a form of compulsive-like behavior in rodents (Welch et al., 2007; Ahmari et al., 2013). In the assessment of behavioral repetition, mice were subjected to repeated stimulation of D_2 receptors with a daily injection of QNP (1 mg/kg), and spontaneous behavior was monitored for 10 min (Fig. 1*A*,*D*,*E*; Movie 1). As previously reported (Asaoka et al., 2019), WT mice, which received repeated stimulation of D_2 receptors (sensitized group; Sens), exhibited repetitive chewing behavior, whereas the saline-treated group (Control) and single stimulation group (Single) did not (Fig. 1*C*). This chewing behavior was similar to a part of nest-building behaviors, but sensitized mice rarely showed other nest-building behaviors (e.g., digging and carrying the cage bedding) during experiments (Fig. 1*F*). In *Nox1* KO mice, sensitization-induced chewing behavior was significantly ameliorated (Fig. 1*F*). Compared with WT-sensitized mice, KO-sensitized mice showed shorter durations of chewing bouts (Fig. 1*G*). A substitution to other repetitive behavior(s) was not observed in any treatment group (Fig. 1*H*). Similarly, when a blood–brain barrier-permeable NOX1 inhibitor, ML171 (50 mg/kg), was acutely injected into WT-sensitized mice 5 min before the last injection of QNP, total chewing time and chewing bout duration both significantly decreased (Fig. 1*I*–*K*).

Perseveration is suggested to be one of the causes of compulsive repetitive behaviors, especially in patients with OCD (MacDonald and Davey, 2005). Perseverative behavior in the reversal learning task, which reflects cognitive inflexibility, is observed both in patients with OCD and addiction (Moreno-López et al., 2015; Tezcan et al., 2017). Consistently, we reported that sensitized mice showed delayed reversal learning in a spatial discrimination task, which may reflect cognitive inflexibility (Asaoka et al., 2019). In this context, we assessed whether NOX1 contributes to the reversal learning deficit in sensitized mice (Fig. 2*A*). Under drug-naive conditions (WT/KO Control; Fig. 2*B*–*D*), *Nox1* deficiency did not affect the performance of the spatial discrimination and its reversal. In sensitized groups (WT/KO Sens; Fig. 2*E*–*G*), which received daily injection of QNP during the overtraining and reversal learning phases, *Nox1* deficiency significantly improved the performance of the reversal learning task (Fig. 2*G*). These results suggest that NOX1 contributes to compulsive behavior repetition and perseveration induced by repeated stimulation of D_2 receptors.

Nox1 was upregulated in the CS of sensitized mice

Dysfunctions in the cortico-striato-thalamo-cortical (CSTC) circuit are responsible for compulsive behaviors (Baxter et al., 1987; Graybiel and Rauch, 2000). To identify the brain regions

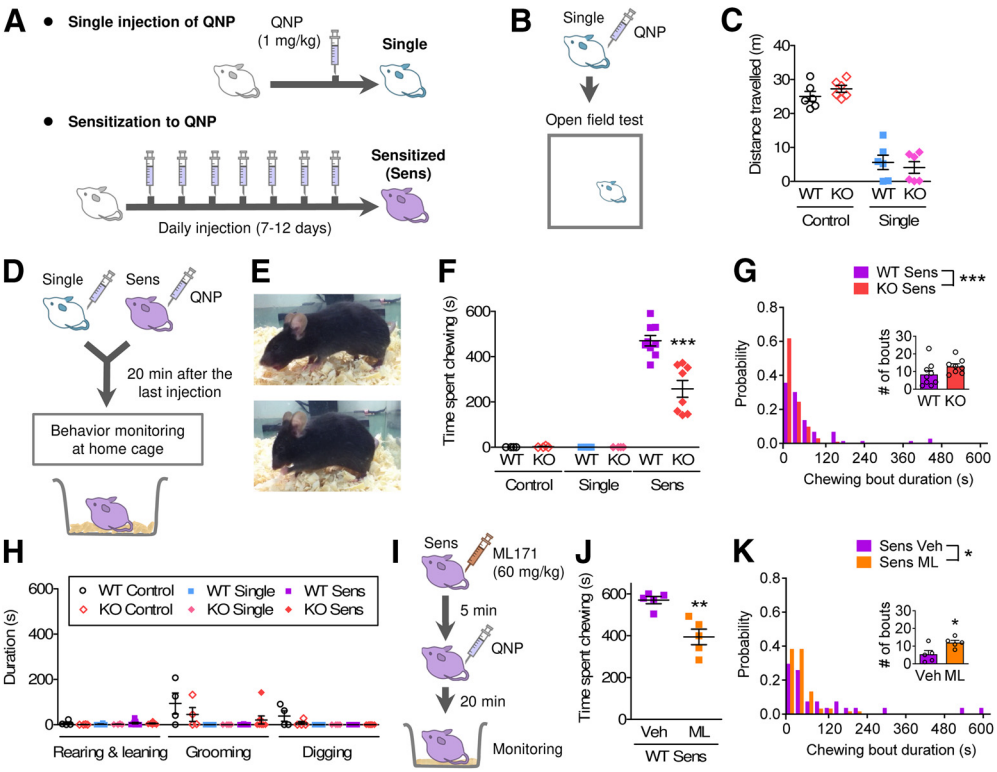

Figure 1. *Nox1* deficiency ameliorated behavioral repetition induced by repeated D_2 receptor stimulation. ***A***, Schematic diagram of the experimental protocol. Mice that received 7-12 daily injections of QNP were referred to as sensitized mice (Sens). ***B***, ***C***, Effects of single D_2 receptor stimulation on locomotor activity. $n = 6$. Two-way repeated-measures ANOVA: $F_{(1,20)} = 1.354$, $p = 0.2717$. ***D***, Schematic diagram of the protocol for behavior monitoring. ***E***, Representative images of chewing behavior. The repeated chewing of cage bedding (wood chips) was observed in sensitized mice. ***F***, Time spent chewing in the 20-30 min after the first (Single) or eighth (Sens) QNP injection (1 mg/kg, i.p.). WT Control: $n = 4$; KO Control: $n = 4$; WT Single: $n = 4$; KO Single: $n = 4$; WT Sens: $n = 9$; KO Sens: $n = 8$. One-way ANOVA: $F_{(5,27)} = 61.71$, $p < 0.0001$. Tukey's multiple comparison test: $^{***}p < 0.001$ versus WT Sens. ***G***, Cumulative probability of chewing bout duration. Two-sample Anderson–Darling test: $^{***}p < 0.001$. Inset, The number of chewing bouts. Student's t test: $t_{(15)} = 1.637$, $^{*}p = 0.1224$. ***H***, Other repetitive behavior during the same recording period as in ***F*** and ***G***. ***I–K***, Effects of systemic injection of ML171, a blood–brain barrier-permeable NOX1 inhibitor on repetitive chewing behavior. $n = 5$. ***J***, Unpaired t test with Welch's correction: $t_{(8)} = 4.280$, $^{**}p = 0.0079$. ***K***, Two-sample Anderson–Darling test: $^{*}p = 0.0137$. Inset, The number of chewing bouts. Student's t test: $t_{(8)} = 2.659$, $^{*}p = 0.0288$.

Movie 1. Typical chewing behavior in WT- and *Nox1* KO-sensitized mice after the ninth injection of QNP. WT-sensitized mice showed repetition of the following behaviors: picking up and holding cage bedding (wood chip) in the forelimbs and gently biting/chewing the chip by the mouth. In *Nox1* KO-sensitized mice, the duration of chewing behavior was shorter than that in WT-sensitized mice. [View online]

responsible for the effects of *Nox1* deficiency on repetitive behavior, we examined the mRNA expression profiles of NOX subtypes in the CSTC-circuit-related brain regions of drug-naive mice by real-time qRT-PCR (Fig. 3*A*). Among the NOX subtypes in the CNS, only the expression levels of *Nox1* mRNA varied by brain region, whereas *Nox2* and *Nox4* expression levels were uniform, except for *Nox4* in the VTA (Fig. 3*B–D*). *Nox1* mRNA expression levels were ~10- to 70-fold higher in the DS and CS than in other brain regions.

Repeated stimulation of dopamine receptor(s) induces sustained changes in the expression of various genes (McClung and Nestler, 2003; Zhang et al., 2005). To test QNP sensitization-induced changes in NOX mRNA expression, the DS and CS were dissected from sensitized mice at least 12 h after the last stimulation, and mRNA expression was determined by real-time qRT-PCR (Fig. 3*E*,*J*). *Nox1* mRNA expression was significantly upregulated in the CS from sensitized mice, while no apparent change was observed in the DS (Fig. 3*F*,*K*). In both DS and CS, *Nox1* deficiency and sensitization to QNP did not affect the expression levels of *Nox2* or *Nox4* (Fig. 3*G*,*H*,*L*,*M*). Consistent with the previous report (Tokunaga et al., 2012), QNP sensitization did not induce compensatory downregulation of *Drd2* mRNA expression in both WT and KO mice (Fig. 3*I*,*N*). Neither *Nox1* deficiency nor QNP sensitization affected the expression level of the housekeeping gene, *Gapdh* (WT Ctrl [CS], 1.00 ± 0.02; WT Sens [CS], 0.98 ± 0.03; KO Ctrl [CS], 0.93 ± 0.09; KO Sens [CS], 0.95 ± 0.03; values are normalized by that of the WT Ctrl group; $n = 7$-9, $p = 0.7255$ by one-way ANOVA).

Repeated stimulation of D_2 receptors facilitated excitatory inputs to the CS in a NOX1-dependent manner

Based on the enriched expression of *Nox1* mRNA in the CS of sensitized mice, we examined the involvement of NOX1 in the

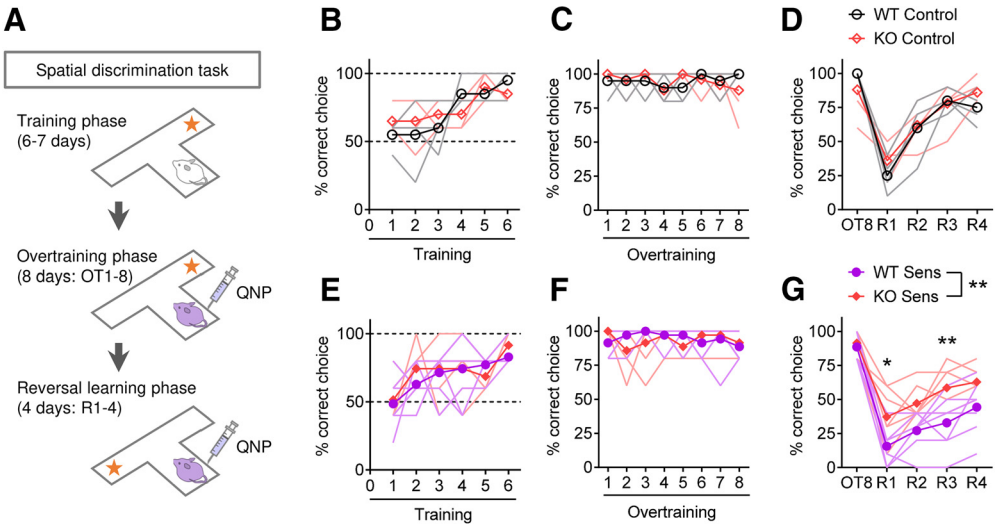

Figure 2. *Nox1* deficiency improved cognitive inflexibility induced by a repeated D_2 receptor stimulation. ***A***, Protocol for the spatial discrimination task and reversal learning test combined with repeated D_2 receptor stimulation. ***B–D***, Percentage of correct choices by drug-naive mice (Control) during the training (***B***), overtraining (***C***), and reversal learning (***D***) periods. $n = 4$. ***B***, Two-way repeated-measures ANOVA: Genotype ($F_{(1,6)} = 0.1017$, $p = 0.7606$), Session number ($F_{(5,30)} = 9.145$, $p < 0.0001$), Interaction ($F_{(5,30)} = 1.572$, $p = 0.1980$). ***C***, Two-way repeated-measures ANOVA: Genotype ($F_{(1,7)} = 0.000$, $p = 1.0000$), Session number ($F_{(7,49)} = 0.866$, $p = 0.5393$), Interaction ($F_{(7,49)} = 1.151$, $p = 0.3480$). ***D***, Two-way repeated-measures ANOVA: Genotype ($F_{(1,7)} = 0.1095$, $p = 0.7503$), Session number ($F_{(4,28)} = 38.95$, $p < 0.0001$), Interaction ($F_{(4,28)} = 1.515$, $p = 0.2247$). ***E–G***, Percentage of correct choices by sensitized mice (Sens) during the training (***E***), overtraining (***F***), and reversal learning (***G***) periods. $n = 6$ or 7. ***E***, Two-way repeated-measures ANOVA: Genotype ($F_{(1,11)} = 0.6371$, $p = 0.4417$), Session number ($F_{(5,55)} = 9.009$, $p < 0.0001$), Interaction ($F_{(5,55)} = 0.5334$, $p = 0.7501$). ***F***, Two-way repeated-measures ANOVA: Genotype ($F_{(1,11)} = 0.2694$, $p = 0.6140$), Session number ($F_{(7,77)} = 0.6227$, $p = 0.7356$), Interaction ($F_{(7,77)} = 2.077$, $p = 0.0560$). ***G***, Two-way repeated-measures ANOVA: Genotype ($F_{(1,11)} = 15.70$, $p = 0.0022$), Session number ($F_{(4,44)} = 41.85$, $p < 0.0001$), Interaction ($F_{(4,44)} = 1.582$, $p = 0.1959$). Bonferroni post-test: $^*p < 0.05$; $^{**}p < 0.01$. Lines with and without symbols indicate mean values and individual data points, respectively.

electrophysiological properties of MSNs in the CS. Consistent with the lack of apparent abnormalities in spontaneous behavior and locomotor activity in control KO mice (Fig. 1*C*,*F*,*H*), *Nox1* deficiency did not affect firing activity (Fig. 4*A–C*,*H–J*), membrane properties (Fig. 4*D*,*E*,*K*,*L*), or spontaneous excitatory inputs (Fig. 4*F*,*G*,*M*,*N*) in iMSNs and dMSNs of naive mice, except for slight but significant interaction effect (genotype × current) in firing activity of iMSNs (Fig. 4*C*).

An increasing number of studies have suggested that hyperactivity of the associative CSTC pathway, including the OFC-striatum pathway, contributes to compulsivity (Ahmari et al., 2013; Hu et al., 2019). Previously, we reported the time dependency of repetitive chewing behavior in WT-sensitized mice. Before the injection of QNP, sensitized mice did not show any chewing behavior. After injection, chewing behavior was transiently observed and it almost disappeared 60 min later (Asaoka et al., 2019). These observations suggest that D_2 receptor stimulation is a trigger for the induction of repetitive behavior in sensitized mice. In addition, consistent with the difference between behavioral responses induced by the first stimulation of D_2 receptors (i.e., sedation) and those induced by stimulation of D_2 receptors after repeated exposure of QNP (i.e., repetitive behavior), synaptic responses to D_2 receptor stimulation were also different between the first stimulation and stimulation after sensitization (Asaoka et al., 2019). Consistent with our previous observations (Asaoka et al., 2019), first *in vitro* exposure to QNP did not affect excitatory inputs in CS iMSN from drug-naive WT mice, whereas, in CS iMSNs from WT-sensitized mice, *in vitro* exposure to QNP significantly facilitated excitatory inputs (Fig. 5*A–C*). In contrast, the facilitating effect of QNP was suppressed by *Nox1* deficiency (Fig. 5*B*). Similarly, when a NOX1 inhibitor, ML171, was bath-applied, subsequent application of QNP did not affect the AMPA/NMDA ratio in iMSNs of WT-sensitized mice (Fig. 5*E*,*F*). Of note, there was no difference in baseline ("Pre") AMPA/NMDA ratios among treatments and genotypes. As for dMSNs, *in vitro* D_2 receptor stimulation did not show any significant effect on eEPSC amplitude (Fig. 5*D*).

Since D_2 receptors are $G_{i/o}$-coupled GPCR, which generally repress synaptic transmission (Shen et al., 2008), we hypothesized that non-G-protein signaling, such as β-arrestin recruitment, may be involved in the synaptic facilitation observed in sensitized mice (Pierce and Lefkowitz, 2001). To test this hypothesis, a β-arrestin-biased D_2 receptor agonist, UNC9994 (UNC), was bath-applied instead of QNP (Fig. 5*G*). Similar to the effects observed following the application of QNP, UNC significantly increased the AMPA/NMDA ratio in iMSNs of WT-sensitized mice, but not in KO-sensitized mice (Fig. 5*H*).

In the striatum, D_2 receptors are also expressed in dopaminergic nerve terminals and striatal interneurons (Calabresi et al., 2014). To examine the contribution of β-arrestin recruitment to the recorded iMSN itself, a β-arrestin inhibitor, barbadin, was applied through the patch pipette to transfer the inhibitor directly into the recorded cell (Fig. 5*I*). In the presence of barbadin, bath application of QNP did not cause any significant change in AMPA/NMDA ratio in iMSNs of WT-sensitized mice (Fig. 5*J*).

Among intracellular signaling molecules activated following β-arrestin recruitment, Src kinase has been reported to play a role in β-arrestin-mediated receptor internalization and initiation of intracellular signaling (Luttrell and Lefkowitz, 2002). A previous study demonstrated that Src-mediated signaling downstream of agonist-induced β-arrestin recruitment plays a role in synaptic plasticity in the hippocampus (Eng et al., 2016). Consistently, when a Src inhibitor, PP2, was applied intracellularly, D_2 receptor stimulation did not cause any increase in AMPA/NMDA ratio in iMSNs of WT-sensitized mice (Fig. 5*K*). Together, these results suggest that, in iMSNs of sensitized mice, NOX1 contributes to synaptic facilitation induced by D_2 receptor stimulation and subsequent recruitment of β-arrestin.

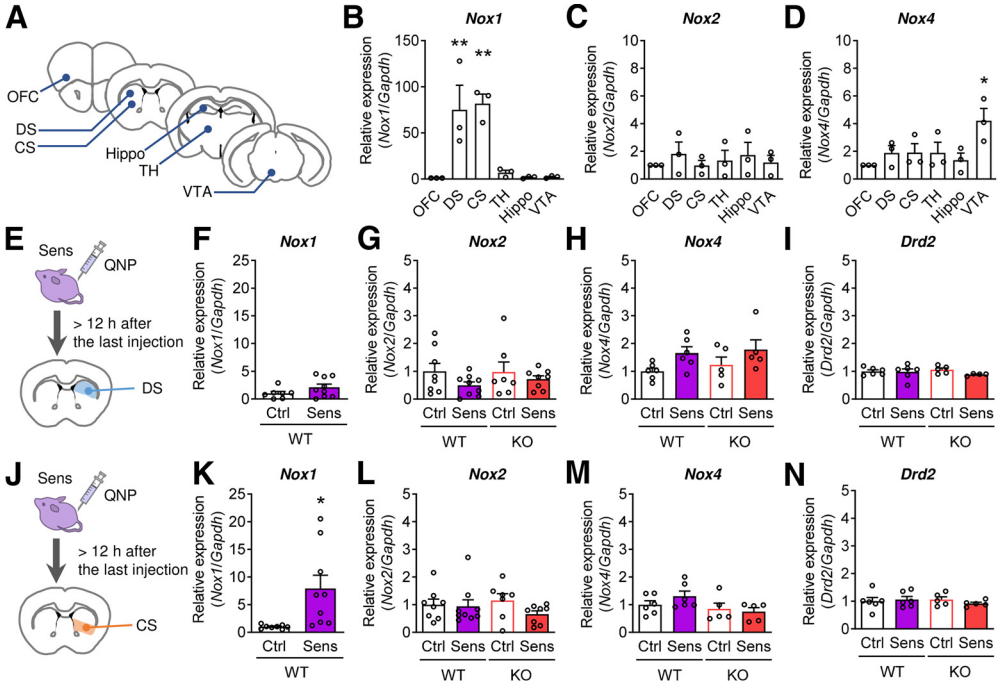

Figure 3. Repeated D_2 receptor stimulation upregulated *Nox1* mRNA expression in a striatal region-specific manner. ***A–D***, Relative expression levels of *Nox1* (***B***), *Nox2* (***C***), and *Nox4* (***D***) mRNAs in the CSTC circuit and related brain regions shown in ***A***. Each sample was obtained from drug-naive mice. $n = 3$. ***B***, One-way ANOVA: $F_{(6,14)} = 10.52$, $p = 0.0002$; Tukey's multiple comparison test: $^{**}p < 0.01$ versus OFC. ***C***, One-way ANOVA: $F_{(6,14)} = 0.2269$, $p = 0.9611$. ***D***, One-way ANOVA: $F_{(6,14)} = 2.987$, $p = 0.0429$; Tukey's multiple comparison test: $^{*}p < 0.05$ versus OFC. ***E–I***, Relative expression levels of *Nox1* (***F***), *Nox2* (***G***), *Nox4* (***H***), and *Drd2* (***I***) mRNAs in the DS from sensitized mice (Sens). $n = 4$-9. ***F***, Student's *t* test: $t_{(14)} = 1.497$, $p = 0.1566$. ***G***, One-way ANOVA: $F_{(3,31)} = 1.070$, $p = 0.3776$. ***H***, One-way ANOVA: $F_{(3,21)} = 2.156$, $p = 0.1287$. ***I***, One-way ANOVA: $F_{(3,20)} = 0.7442$, $p = 0.5404$. ***J–N***, Relative expression levels of *Nox1* (***K***), *Nox2* (***L***), *Nox4* (***M***), and *Drd2* (***N***) mRNAs in the CS from Sens mice. $n = 5$-9. ***K***, Unpaired *t* test with Welch's correction: $t_{(14)} = 2.881$, $p = 0.0205$. ***L***, One-way ANOVA: $F_{(3,31)} = 0.9343$ $p = 0.4372$. ***M***, One-way ANOVA: $F_{(3,18)} = 2.000$, $p = 0.1501$. ***N***, One-way ANOVA: $F_{(3,21)} = 0.3562$, $p = 0.7853$.

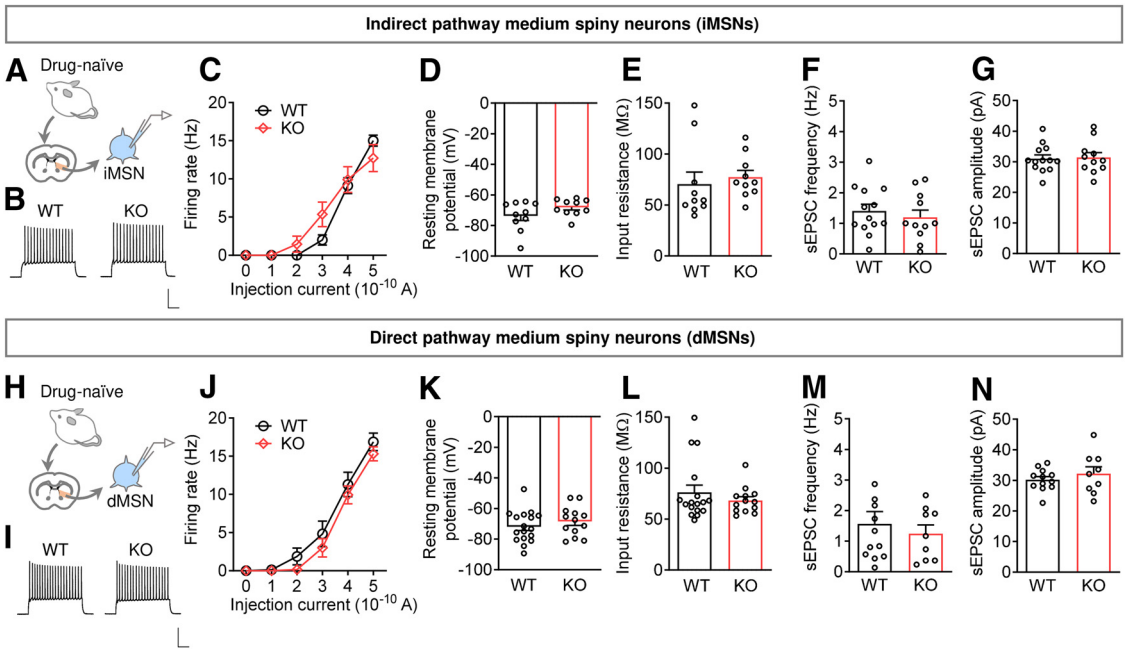

Figure 4. *Nox1* deficiency did not affect basal electrophysiological properties of both iMSNs and dMSNs in the CS. ***A–C***, Firing activity elicited by current injection in CS iMSNs of drug-naive mice. ***B***, Calibration: 100 ms, 50 mV. ***C***, $n = 10$ from 5 mice. Two-way repeated-measures ANOVA: Genotype ($F_{(1,19)} = 0.3306$, $p = 0.5721$), Current ($F_{(5,95)} = 97.41$, $p < 0.0001$), Interaction ($F_{(5,95)} = 2.518$, $p = 0.0347$). ***D***, ***E***, Resting membrane potential (***D***) and input resistance (***E***) of CS iMSNs from drug-naive mice. $n = 10$ from 5 mice. ***D***, Student's *t* test: $t_{(10)} = 1.579$, $p = 0.1318$. ***E***, Student's *t* test: $t_{(18)} = 0.5050$, $p = 0.6197$. ***F***, ***G***, Spontaneous EPSC frequency (***F***) and amplitude (***G***) in CS iMSNs from drug-naive mice. $n = 11$-13 from 7 or 8 mice. ***F***, Student's *t* test: $t_{(22)} = 0.6448$, $p = 0.5257$. ***G***, Student's *t* test: $t_{(22)} = 0.2057$, $p = 0.8389$. ***H–J***, Firing activity elicited by the current injection in CS dMSNs of drug-naive mice. ***I***, Calibration: 100 ms, 50 mV. ***J***, $n = 13$-17 from 5 mice. Two-way repeated-measures ANOVA: Genotype ($F_{(1,28)} = 0.9674$, $p = 0.3338$), Current ($F_{(5,140)} = 156.4$, $p < 0.0001$), Interaction ($F_{(5,140)} = 0.6014$, $p = 0.6989$). ***K***, ***L***, Resting membrane potential (***K***) and input resistance (***L***) of CS dMSNs from drug-naive mice. $n = 13$-17 from 5 mice. ***K***, Student's *t* test: $t_{(28)} = 0.9398$, $p = 0.3553$. ***L***, Student's *t* test: $t_{(28)} = 0.9176$, $p = 0.3667$. ***M***, ***N***, Spontaneous EPSC frequency (***M***) and amplitude (***N***) in CS dMSNs from drug-naive mice. $n = 9$-12 from 8 mice. ***M***, Student's *t* test: $t_{(19)} = 0.6044$, $p = 0.5527$. ***N***, Student's *t* test: $t_{(19)} = 0.8661$, $p = 0.3972$.

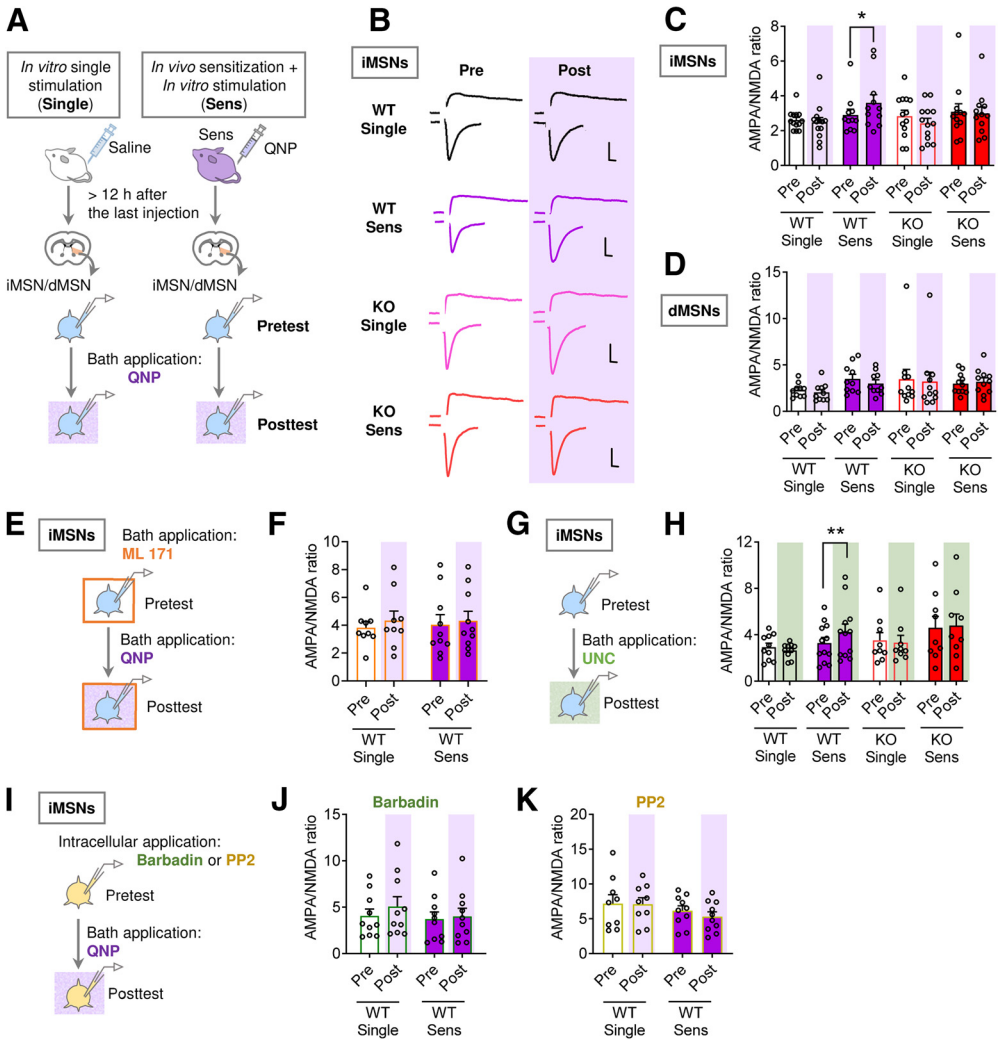

Figure 5. Repeated stimulation of D_2 receptors facilitated excitatory inputs to the CS in a NOX1-dependent manner. ***A***, Schematic diagram of the experimental protocol. ***B***, ***C***, The AMPA/NMDA ratio was recorded from CS iMSNs before and after bath application of QNP (10 μM). Representative traces are shown in ***B***. Calibration: 5 ms, 500 pA. ***C***, $n = 11$-13 from 6-11 mice. Three-way repeated-measures ANOVA: Pre-Post ($F_{(1,45)} = 0.02340$, $p = 0.8791$), Sensitization ($F_{(1,45)} = 2.983$, $p = 0.0910$), Genotype ($F_{(1,45)} = 0.03614$, $p = 0.8501$), Pre-Post × Sensitization ($F_{(1,45)} = 7.488$, $p = 0.0089$), Pre-Post × Genotype ($F_{(1,45)} = 6.690$, $p = 0.0130$), Sensitization × Genotype ($F_{(1,45)} = 0.2053$, $p = 0.6527$), Pre-Post × Sensitization × Genotype ($F_{(1,45)} = 1.414$, $p = 0.2407$). Sidak's multiple comparisons test: $^*p < 0.05$. ***D***, The AMPA/NMDA ratio was recorded from CS dMSNs before and after bath application of QNP (10 μM). $n = 10$ or 11 from 7-10 mice. Three-way repeated-measures ANOVA: Pre-Post ($F_{(1,38)} = 0.1673$, $p = 0.1673$), Sensitization ($F_{(1,38)} = 0.4755$, $p = 0.4947$), Genotype ($F_{(1,38)} = 0.6889$, $p = 0.4117$), Pre-Post × Sensitization ($F_{(1,38)} = 0.1492$, $p = 0.7014$), Pre-Post × Genotype ($F_{(1,38)} = 1.596$, $p = 0.2142$), Sensitization × Genotype ($F_{(1,38)} = 1.190$, $p = 0.2822$), Pre-Post × Sensitization × Genotype ($F_{(1,38)} = 1.545$, $p = 0.2215$). ***E***, ***F***, In the presence of a NOX1 inhibitor, ML171 (5 μM), the AMPA/NMDA ratio was recorded from CS iMSNs before and after bath application of QNP (10 μM). ***F***, $n = 9$ or 10 from 5 or 6 mice. Two-way repeated-measures ANOVA: Pre-Post ($F_{(1,17)} = 2.789$, $p = 0.1132$), Sensitization ($F_{(1,17)} = 0.01199$, $p = 0.9141$), Interaction ($F_{(1,17)} = 0.2266$, $p = 0.6401$). ***G***, ***H***, The AMPA/NMDA ratio was recorded from CS iMSNs before and after bath application of UNC9994 (UNC; 10 μM), an arrestin-biased D_2 receptor agonist. ***H***, $n = 9$-12 from 5-8 mice. Three-way repeated-measures ANOVA: Pre-Post ($F_{(1,36)} = 1.442$, $p = 0.2377$), Sensitization ($F_{(1,36)} = 3.095$, $p = 0.0870$), Genotype ($F_{(1,36)} = 1.484$, $p = 0.2310$), Pre-Post × Sensitization ($F_{(1,36)} = 8.477$, $p = 0.0061$), Pre-Post × Genotype ($F_{(1,36)} = 1.443$, $p = 0.2375$), Sensitization × Genotype ($F_{(1,36)} = 0.05931$, $p = 0.8090$), Pre-Post × Sensitization × Genotype ($F_{(1,36)} = 2.255$, $p = 0.1419$). Sidak's multiple comparisons test: $^{**}p < 0.01$. ***I–K***, Following the intracellular application of barbadin, a β-arrestin inhibitor (***J***; 100 μM) or PP2, a Src kinase inhibitor (***K***; 1 μM), the AMPA/NMDA ratio was recorded from CS iMSNs before and after bath application of QNP. ***J***, $n = 10$ from 6 mice. Two-way repeated-measures ANOVA: Pre-Post ($F_{(1,18)} = 3.729$, $p = 0.0694$), Sensitization ($F_{(1,18)} = 0.3481$, $p = 0.5625$), Interaction ($F_{(1,18)} = 1.176$, $p = 0.2924$). ***K***, $n = 9$ or 10 from 5 mice. Two-way repeated-measures ANOVA: Pre-Post ($F_{(1,17)} = 1.930$, $p = 0.1827$), Sensitization ($F_{(1,17)} = 1.295$, $p = 0.2708$), Interaction ($F_{(1,17)} = 1.272$, $p = 0.2750$).

As previously reported, sensitized mice also exhibited increased firing activity of pyramidal neurons in the lOFC (Fig. 6*A*,*B*), which projects to the CS (Asaoka et al., 2019). To evaluate the contribution of NOX1 in the hyperactivity of lOFC pyramidal neurons, we recorded the firing response of lOFC pyramidal neurons in KO Sens mice. Consistent with the low *Nox1* expression levels in the OFC (Fig. 3*C*), *Nox1* deficiency did not improve the sensitization-induced abnormal activity of lOFC pyramidal neurons (Fig. 6*C*). *Nox1* deficiency did not affect resting membrane potential and input resistance, except for the slight depolarized resting membrane potential of the KO control group (Fig. 6*D*,*E*). Together, these results suggest that NOX1 predominantly regulates synaptic abnormalities in the CS rather than lOFC hyperactivity in sensitized mice.

NOX1 was required for the accumulation of activated Src induced by D_2 receptor stimulation in sensitized mice

Next, we examined the potential mechanisms underlying the NOX1-mediated regulation of D_2 receptor signaling in the CS, particularly in relation to the recruitment of β-arrestin. As the main target of ROS, PTPs are reversibly inhibited by the oxidation of cysteine residue at the catalytic site (Meng et al., 2002).

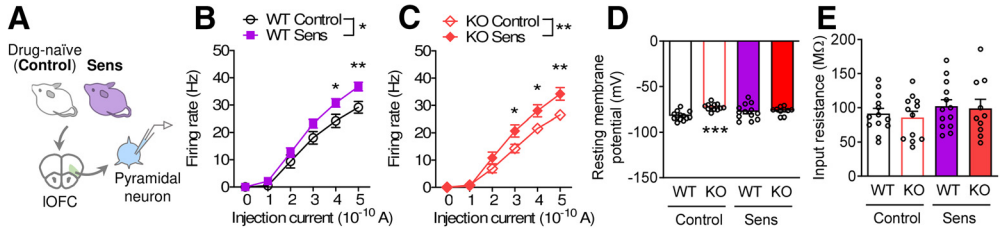

Figure 6. *Nox1* deficiency did not improve lOFC hyperactivity in sensitized mice. ***A–C***, Current injection-induced firing activity of lOFC pyramidal neurons from WT drug-naive (Control) and sensitized (Sens) mice. ***B***, $n = 13$ from 3 mice. Two-way repeated-measures ANOVA: Genotype ($F_{(1,120)} = 4.611$, $p = 0.0421$), Current ($F_{(5,600)} = 324.2$, $p < 0.0001$), Interaction ($F_{(5,600)} = 3.697$, $p = 0.0038$). Bonferroni post-test: $^{*}p < 0.05$; $^{**}p < 0.01$. ***C***, $n = 10$-12 from 3 mice. Two-way repeated-measures ANOVA: Genotype ($F_{(1,100)} = 6.359$, $p = 0.0203$), Current ($F_{(5,500)} = 288.5$, $p < 0.0001$), Interaction ($F_{(5,500)} = 5.540$, $p = 0.0002$). Bonferroni post-test: $^{*}p < 0.05$; $^{**}p < 0.01$. ***D***, ***E***, Resting membrane potential (***D***) and input resistance (***E***) of lOFC pyramidal neurons from WT drug-naive (Control) and sensitized (Sens) mice. $n = 10$-13 from 3 mice. ***D***, One-way ANOVA: $F_{(3,44)} = 6.351$, $p = 0.0011$. Tukey's multiple comparison test: $^{***}p < 0.001$ versus WT Control. ***E***, one-way ANOVA: $F_{(3,44)} = 0.5891$, $p = 0.6254$.

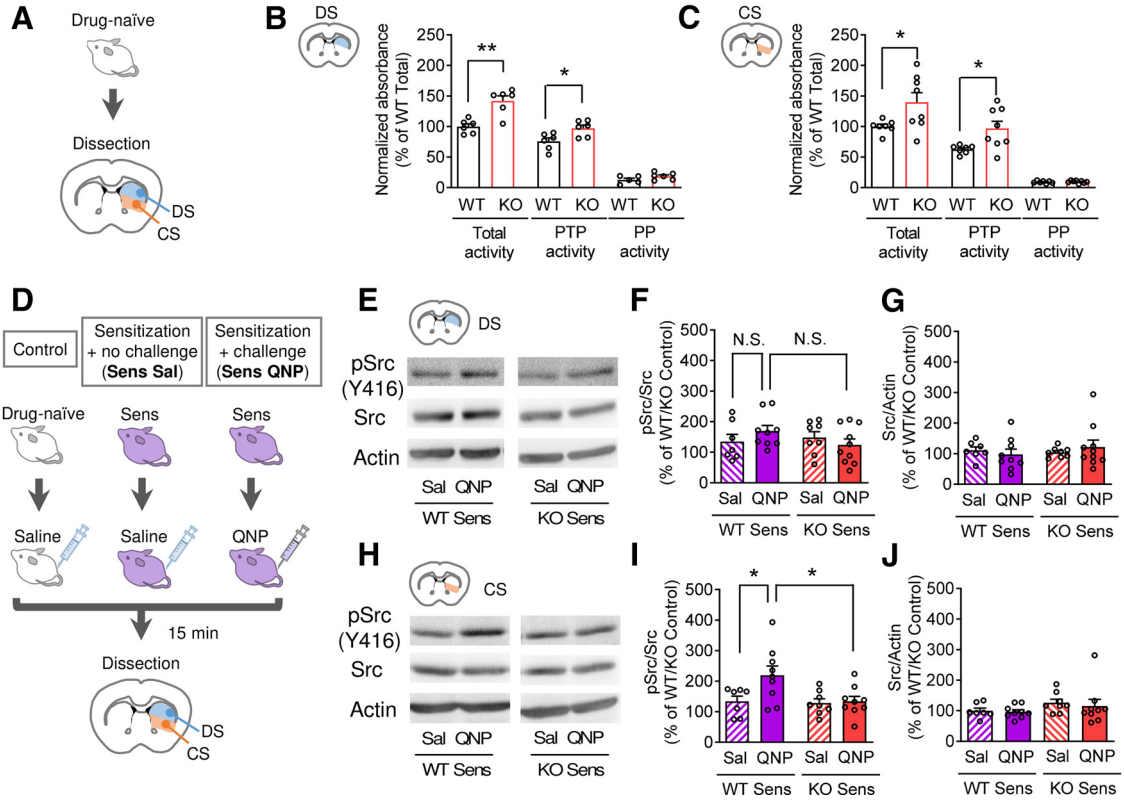

Figure 7. NOX1 was required for the accumulation of activated Src induced by D_2 receptor stimulation in sensitized mice. ***A–C***, Phosphatase activity of the DS (***B***) and CS (***C***) from drug-naive mice. Values are normalized by that of the WT Total group of each region. ***B***, $n = 5$ or 6. Total: unpaired t test with Welch's correction: $t_{(7)} = 4.368$, $^{**}p = 0.0033$; PTP: unpaired t test with Welch's correction: $t_{(9)} = 2.770$, $^{*}p = 0.0218$; PP: Student's t test: $t_{(9)} = 0.1416$, $p = 0.1416$. ***C***, $n = 7$ or 8. Total: unpaired t test with Welch's correction: $t_{(7)} = 2.475$, $^{*}p = 0.0425$; PTP: unpaired t test with Welch's correction: $t_{(7)} = 2.850$, $^{*}p = 0.0247$; PP: Student's t test: $t_{(13)} = 0.4228$, $p = 0.6794$. ***D***, Regarding Western blotting, Sens mice were divided into two groups and challenged with saline (Sens Sal) or QNP (Sens QNP) 15 min before the dissection of the DS and CS. ***E–J***, Western blot analyses of phosphorylation of Src Y416 in the DS (***E–G***) and CS (***H–J***). The values are normalized by that of the respective control mice of each genotype. ***F***, $n = 7$-9. Two-way ANOVA: Genotype ($F_{(1,30)} = 0.06535$, $p = 0.8004$), Challenge ($F_{(1,30)} = 0.2191$, $p = 0.6431$), Interaction ($F_{(1,30)} = 3.123$, $p = 0.0874$). N.S.: not significant. ***G***, $n = 7$-9. Two-way ANOVA: Genotype ($F_{(1,30)} = 0.2599$, $p = 0.6139$), Challenge ($F_{(1,30)} = 0.01137$, $p = 0.9158$), Interaction ($F_{(1,30)} = 0.8137$, $p = 0.3742$). ***I***, $n = 7$-9. Two-way ANOVA: Genotype ($F_{(1,29)} = 4.564$, $p = 0.0412$), Challenge ($F_{(1,29)} = 4.523$, $p = 0.0421$), Interaction ($F_{(1,29)} = 3.532$, $p = 0.0703$). Bonferroni post-test: $^{*}p < 0.05$. ***J***, $n = 7$-9. Two-way ANOVA: Genotype ($F_{(1,29)} = 2.462$, $p = 0.1275$), Challenge ($F_{(1,29)} = 0.2305$, $p = 0.6348$), Interaction ($F_{(1,29)} = 0.05911$, $p = 0.8096$).

To confirm the inhibitory effect of NOX1-derived ROS on striatal PTP activity under physiological conditions, we measured phosphatase activity in the DS and CS of drug-naive mice (Fig. 7*A*). In both the DS (Fig. 7*B*) and CS (Fig. 7*C*), *Nox1* deficiency significantly increased total phosphatase and PTP activities without affecting serine-threonine phosphatase (PP) activity. Compared with WT DS, WT CS exhibited higher phosphatase activity (WT DS, 100.0 ± 4.53%, $n = 6$; WT CS, 138.5 ± 6.42%; values are normalized by that of the WT DS group, $n = 6$; $p = 0.0012$ by Student's t test).

NOX1-mediated inhibition of PTP activity may potentiate tyrosine phosphorylation signaling by delaying the dephosphorylation reaction. Since behavioral abnormalities and synaptic facilitation in sensitized mice were only elicited after the challenge with QNP, NOX1-mediated potentiation of phosphorylation signaling followed by D_2 receptor stimulation in sensitized mice may be key in the provocation of repetitive behavior and electrophysiological abnormalities. To test this idea, we dissected the DS and CS from sensitized mice 15 min after an injection of saline (Sens Sal) or QNP (Sens QNP; Fig. 7*D*) and measured Src

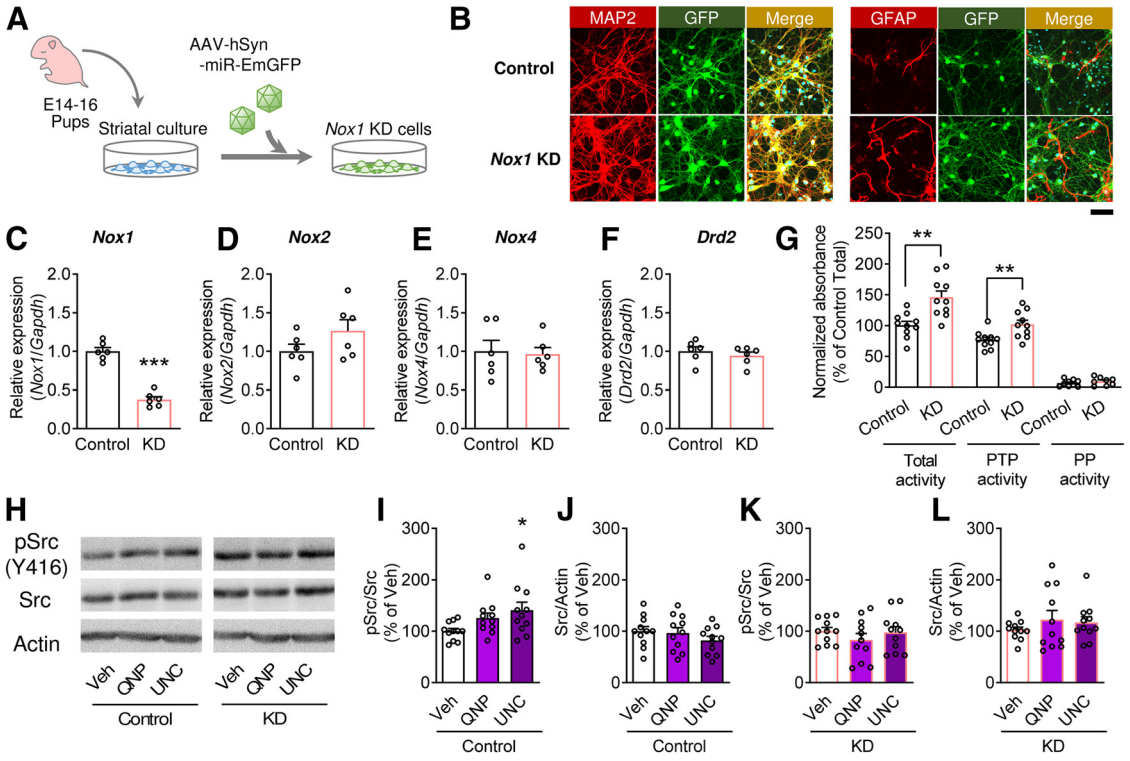

Figure 8. NOX1 was required for the accumulation of activated Src induced by D_2 receptor stimulation in primary cultured striatal neurons. ***A***, AAV-miRNA-mediated *Nox1* KD in primary cultures of mouse striatal neurons. ***B***, Representative images of immunostaining. Red represents MAP2, a marker for neurons; or GFAP, a marker for astrocytes. Green represents EmGFP, depicting miRNA-expressing cells. Cyan represents DAPI. Scale bar, 50 μm. ***C–F***, Relative expression levels of *Nox1* (***C***), *Nox2* (***D***), *Nox4* (***E***), and *Drd2* (***F***) mRNAs in striatal cultures 7 d after AAV infection; $n = 6$. ***C***, Student's *t* test: $t_{(10)} = 10.17$, $p < 0.0001$. ***D***, Student's *t* test: $t_{(10)} = 1.558$, $p = 0.1502$. ***E***, Student's *t* test: $t_{(10)} = 0.2264$, $p = 0.8254$. ***F***, Student's *t* test: $t_{(10)} = 0.7681$, $p = 0.4602$. ***G***, Phosphatase activity of AAV-infected neuronal cultures. The values are normalized by that of the Control Total group. $n = 9$ or 10; Total: Student's *t* test: $t_{(18)} = 3.771$, $^{**}p = 0.0014$; PTP: Student's *t* test: $t_{(18)} = 3.030$, $^{**}p = 0.0072$; PP: Student's *t* test: $t_{(15)} = 0.9569$, $p = 0.3538$. ***H–L***, Western blot analyses of phosphorylation of Src Y416 in neuronal cultures infected with control AAV (***I***,***J***) or with AAV-miRNA (***K***,***L***) after an incubation in the presence of vehicle (Veh), QNP (1 μM), or UNC (1 μM) for 20 min. The values are normalized by that of the Veh group. ***I***, $n = 11$. One-way ANOVA: $F_{(2,32)} = 3.445$, $p = 0.0450$; Tukey's multiple comparison test: $^{*}p < 0.05$ versus Veh. ***J***, $n = 11$. One-way ANOVA: $F_{(2,32)} = 1.060$, $p = 0.3591$. ***K***, $n = 11$. One-way ANOVA: $F_{(2,32)} = 0.7293$, $p = 0.4906$. ***L***, $n = 11$. One-way ANOVA: $F_{(2,32)} = 0.6784$, $p = 0.5151$.

phosphorylation at tyrosine 416 (Y416). In the DS, both WT Sens Sal and Sens QNP groups showed a moderate increase in Src phosphorylation from that in the control group (WT Sens Sal, 135.0 ± 23.77%; WT Sens QNP, 169.3 ± 18.45%); however, no significant differences were observed between the groups (Fig. 7*E–G*). In the CS (Fig. 7*H–J*), the WT Sens Sal group showed a slight increase in Src phosphorylation than the control group, and QNP injection induced the further accumulation of phosphorylated Src (WT Sens Sal, 134.1 ± 17.08%; WT Sens QNP, 219.5 ± 30.26%). In *Nox1* KO-sensitized mice, QNP-induced increases in phosphorylated Src were not observed, suggesting a critical role for NOX1 in the D_2 receptor stimulation-induced Src activation in the CS of sensitized mice.

NOX1 was required for the accumulation of activated Src induced by D_2 receptor stimulation *in vitro*

We assessed the contribution of NOX1 and D_2 receptors in striatal neurons to the accumulation of activated Src using primary cultures of mouse striatal neurons. For the neuron-specific *Nox1* knockdown (KD), cells were treated with AAV, which expresses miRNA for *Nox1* and EmGFP under the control of the hSyn promoter (Fig. 8*A*,*B*). One week after AAV infection, *Nox1* expression levels decreased by up to 35% (Fig. 8*C*), whereas those of *Nox2*, *Nox4*, and *Drd2* were unaffected (Fig. 8*D–F*). *Nox1* KD did not affect the expression level of the housekeeping gene, *Gapdh* (Ctrl, 1.00 ± 0.02; KD, 1.02 ± 0.03; values were normalized by that of Ctrl, $n = 6$, $t_{(5)} = 0.7339$, $p = 0.4919$ by unpaired *t* test with Welch's correction). Consistent with the results from *Nox1* KO mice, neuron-specific *Nox1* KD significantly increased total phosphatase and PTP activities in primary cultures of mouse striatal neurons (Fig. 8*G*).

Under *in vitro* conditions, a single, but prolonged, stimulation of D_2 receptors facilitates Src phosphorylation via the recruitment of β-arrestin (Huang et al., 2013). When striatal cultures were stimulated by QNP for 20 min, phosphorylation of Src Y416 showed a slight increase. The phosphorylation of Src was further increased by stimulation with UNC (Fig. 8*H–J*), whereas QNP and UNC did not exert any effect on *Nox1* KD cells (Fig. 8*K*,*L*). These results confirmed that NOX1 is required for Src activation induced by D_2 receptor stimulation and subsequent β-arrestin recruitment.

We also examined the effects of NOX1 overexpression (OE) on receptor internalization and the accumulation of activated Src. HEK 293T cells were cotransfected with FLAG-tagged hDRD2, hNOX1, and auxiliary subunits (hNOXO1 and hNOXA1) (Fig. 9*A*). To assess the agonist-induced internalization of D_2 receptors, FLAG-hDRD2 was labeled with a FLAG-specific antibody just before QNP treatment. In the mock-transfected group, which was transfected with FLAG-hDRD2, hNOXO1, hNOXA1, and mock vector, FLAG-hDRD2 immunoreactivity was mainly observed at the plasma membrane region (PHA-L binding region), whereas significant strong immunoreactivity was observed in the intracellular region of NOX1 OE cells treated with QNP, compared with mock-transfected cells

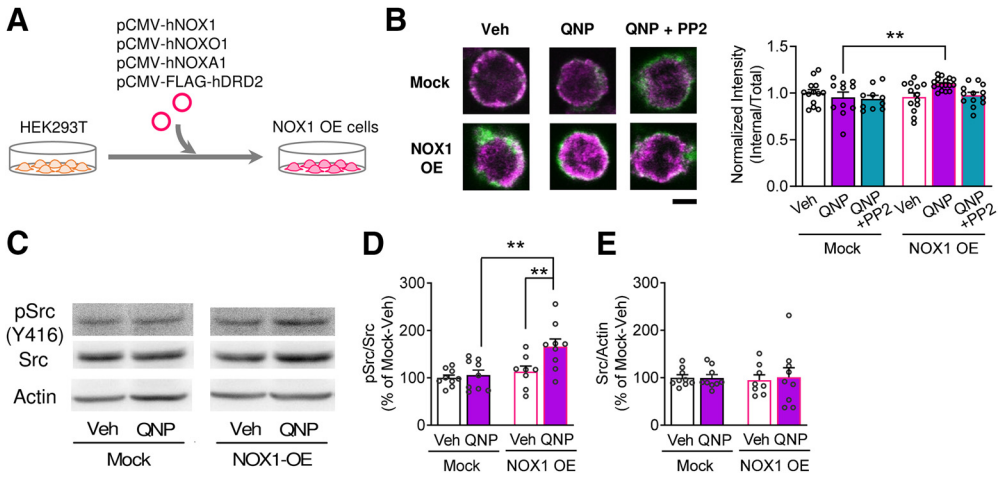

Figure 9. Overexpression of NOX1 facilitated agonist-induced D_2 receptor internalization and accumulation of activated Src. ***A***, HEK293T cells were transfected with plasmids encoding hNOX1, hNOXO1, hNOXA1, and FLAG-tagged hDRD2. ***B***, Left, Representative images for the immunostaining of hDRD2-expressing HEK293T cells after a 20 min incubation with vehicle (Veh), QNP (1 μM), or QNP + PP2 (1 μM). Green represents PHA-L (plasma membrane). Magenta represents FLAG-DRD2. Scale bar, 10 μm. Right, Quantitative data for internalization of D_2 receptors. Values are normalized by that of the Mock-Veh group. $n = 13$-17. Two-way ANOVA: Overexpression ($F_{(1,79)} = 4.843$, $p = 0.0041$), Drug ($F_{(2,79)} = 0.6580$, $p = 0.5207$), Interaction ($F_{(2,79)} = 5.192$, $p = 0.0076$). Bonferroni post-test: $^{**}p < 0.01$ versus Mock-QNP. ***C–E***, Western blot analysis of phosphorylation of Src Y416. Values are normalized by that of the Mock-Veh group. $n = 8$ or 9. ***D***, Two-way ANOVA: Overexpression ($F_{(1,31)} = 9.618$, $p = 0.0041$), Drug ($F_{(1,31)} = 6.236$, $p = 0.0180$), Interaction ($F_{(1,31)} = 3.974$, $p = 0.0551$). Bonferroni post-test: $^{**}p < 0.01$. ***E***, Two-way ANOVA: Overexpression ($F_{(1,31)} = 0.01911$, $p = 0.8909$), Drug ($F_{(1,31)} = 0.04204$, $p = 0.8389$), Interaction ($F_{(1,31)} = 0.06882$, $p = 0.7948$).

treated with QNP (Fig. 9*B*), suggesting that NOX1-OE facilitated D_2 receptor internalization. Furthermore, agonist-induced subcellular localization of D_2 receptors was suppressed by cotreatment with a Src inhibitor, PP2, confirming the requirement of Src activation for agonist-induced receptor internalization (Luttrell and Lefkowitz, 2002).

As for Src activation, stimulation with QNP did not increase phosphorylation of Src Y416 in the mock-transfected group (Fig. 9*C–E*), consistent with the data obtained from *Nox1* KO mice and *Nox1* KD striatal cultures. In contrast, QNP significantly increased Src phosphorylation in NOX1-OE cells. Notably, there was no significant change in the Src phosphorylation level between vehicle-treated groups. These results support the idea that NOX1 facilitates the accumulation of activated Src in response to D_2 receptor stimulation.

Inhibition of NOX1 or β-arrestin in the CS is sufficient to ameliorate repetitive behavior

The above results demonstrate that NOX1 upregulation and NOX1-mediated control of D_2 receptor signaling in sensitized mice preferentially occurred in the CS. To confirm that such striatal subregion-specific changes are critical for behavioral repetition in sensitized mice, we investigated the effects of the local inhibition of NOX1 or β-arrestin. WT mice were bilaterally implanted with cannulae into the CS and received a repeated D_2 receptor stimulation (Fig. 10*A*,*B*). Microinjection of a NOX1/4 inhibitor, setanaxib, significantly reduced both the total and bout durations of chewing behavior in sensitized mice (Fig. 10*C–E*). Similar changes were observed following an injection of a β-arrestin inhibitor, barbadin (Fig. 10*F–H*). No substitution to other repetitive behavior(s) was observed in any treatment group (Fig. 10*E*,*H*). Local injection of setanaxib or barbadin did not affect the locomotor activity of drug-naive mice (vehicle, 19.52 ± 2.82 m; setanaxib, 26.61 ± 7.36 m; barbadin, 29.92 ± 4.77 m; $n = 4$, $p = 0.4643$ by one-way repeated-measures ANOVA).

We also assessed the effect of striatal neuron-specific KD of *Nox1* by intrastriatal injection of miRNA-expressing AAV (Fig. 10*I*,*J*,*N*). In sensitized KD mice (KD Sens), repetitive chewing behavior was significantly reduced compared with sensitized mice injected with control AAV (Control Sens) (Fig. 10*K*). The duration of chewing behavior was also shorter in KD Sens mice than that in control Sens mice (Fig. 10*L*). No substitution to other repetitive behavior(s) was observed in either group (Fig. 10*M*). In the spatial discrimination task, KD Sens mice showed similar performance as control Sens mice in the training and overtraining phases (Fig. 10*O*,*P*). In contrast, KD Sens mice exhibited higher performance than control Sens mice in reversal learning task (Fig. 10*Q*), suggesting that striatal neuron-specific KD of *Nox1* was sufficient for improving both repetitive behavior and cognitive inflexibility induced by QNP sensitization.

Collectively, these results indicate the significant contribution of striatal NOX1-mediated control of D_2 receptor signaling to behavioral repetition and cognitive inflexibility.

Discussion

In the present study, we provided the first piece of evidence showing that repeated D_2 receptor stimulation enhanced excitatory synaptic inputs in CS iMSNs and caused repetitive and perseverative behaviors through the recruitment of β-arrestin. The novelty of the present study lies in the regulatory function of NOX1 in D_2 receptor-mediated signaling. By attenuating PTP activity, NOX1 promoted the accumulation of activated Src induced by D_2 receptor stimulation in the CS, resulting in the facilitation of excitatory inputs and progression of behavioral abnormalities reflecting compulsivity (Fig. 11).

Recent evidence indicates the significant involvement of hyperactivation of corticostriatal pathways, as well as abnormal dopaminergic signaling, in various forms of behavioral repetition, such as compulsive behavior (Welch et al., 2007), and involuntary movements, such as dyskinesia (Fieblinger et al., 2014). Among the three functionally different striatal subregions (the motor, associative, and limbic striatum), hyperactivation of the OFC-associative striatum pathway is suggested to be correlated with compulsive repetitive behavior (Ahmari et al., 2013), while abnormal activity in the motor striatum is responsible for involuntary repetitive behavior (Loonen and Ivanova, 2013).

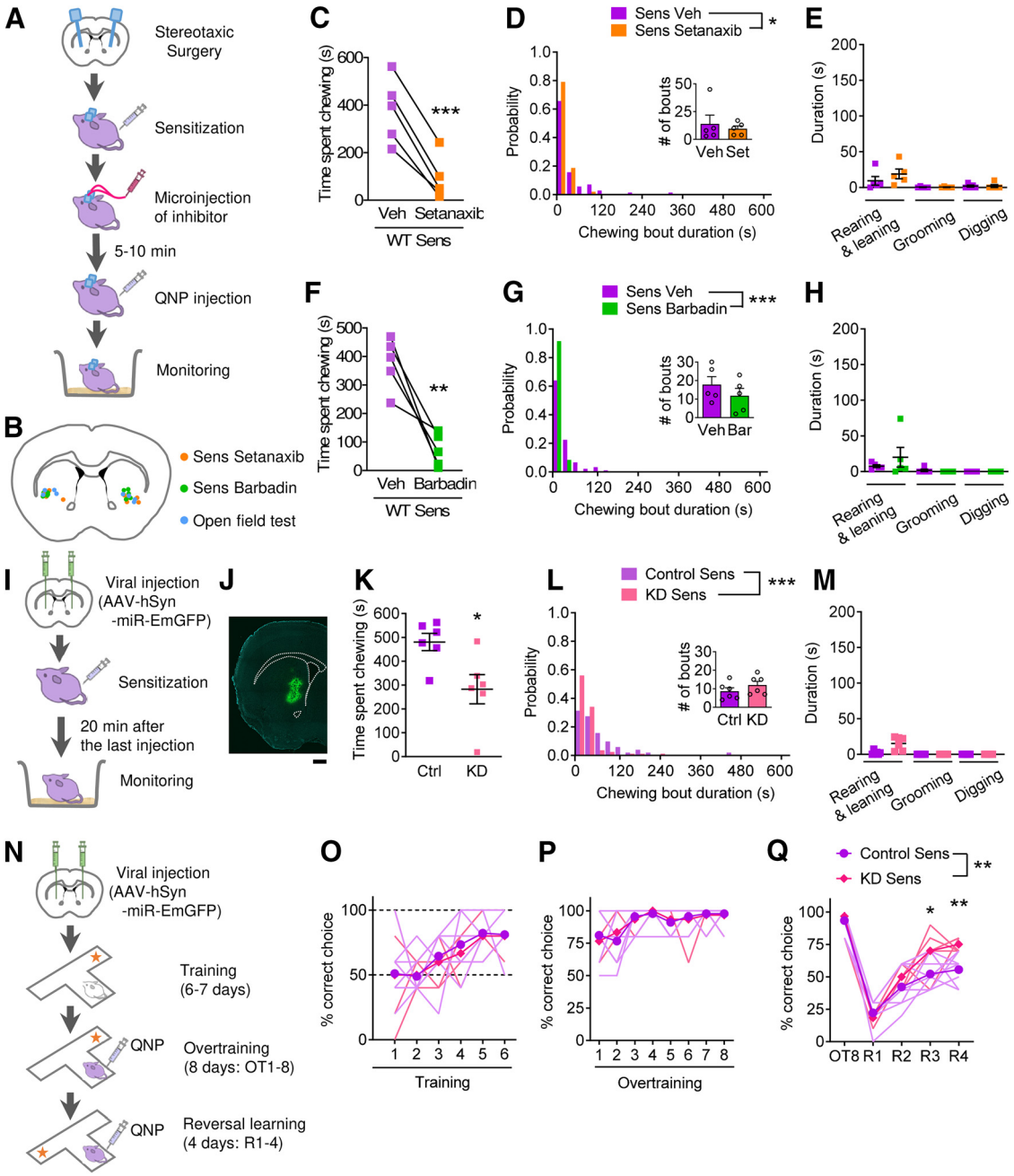

Figure 10. Inhibition of NOX1 or β-arrestin in the CS was sufficient to attenuate repetitive behavior. ***A***, Experimental protocol for stereotaxic surgery and the microinjection of inhibitors for behavior analyses. ***B***, Schematic illustration of cannula placements. ***C***, ***D***, Effects of an injection of setanaxib (1 μg/μl/side) in the CS on repetitive chewing behavior in sensitized mice. ***C***, $n = 5$. Paired t test: $t_{(4)} = 9.131$, $^{***}p = 0.0008$. ***D***, Two-sample Anderson–Darling test: $^{*}p = 0.048$. Inset, The number of chewing bouts. Paired t test: $t_{(4)} = 0.5898$, $p = 0.5870$. ***E***, Other repetitive behaviors during the same recording period as in ***C*** and ***D***. ***F***, ***G***, Effects of an injection of barbadin (1 μg/μl/side) in the CS on repetitive chewing behavior in sensitized mice. ***F***, $n = 5$. Paired t test: $t_{(4)} = 5.091$, $^{**}p = 0.0070$. ***G***, Two-sample Anderson–Darling test: $^{***}p < 0.001$. Inset, The number of chewing bouts. Paired t test: $t_{(4)} = 2.000$, $p = 0.1161$. ***H***, Other repetitive behaviors during the same recording period as in ***F*** and ***G***. ***I***, Experimental protocol for analyzing spontaneous behaviors in striatal neuron-specific *Nox1* KD mice. ***J***, Representative image for the AAV-mediated expression of EmGFP in the striatum. Scale bar, 500 μm. ***K***, ***L***, Time spent chewing in control and *Nox1* KD-sensitized mice. ***K***, $n = 6$. Student's t test: $t_{(10)} = 2.768$, $^{*}p = 0.0198$. ***L***, Two-sample Anderson–Darling test: $^{***}p < 0.001$. Inset, The number of chewing bouts. Student's t test: $t_{(10)} = 1.206$, $p = 0.2557$. ***M***, Other repetitive behaviors during the same recording period as in ***K*** and ***L***. ***N***, Experimental protocol for spatial discrimination task in striatal neuron-specific *Nox1* KD mice. ***O–Q***, Percentage of correct choices by control and *Nox1* KD-sensitized mice (Sens) during the training (***O***), overtraining (***P***), and reversal learning (***Q***) periods. Control: $n = 9$; KD: $n = 6$. ***O***, Two-way repeated-measures ANOVA: *Nox1* KD ($F_{(1,13)} = 0.2582$, $p = 0.6199$), Session number ($F_{(5,65)} = 8.564$, $p < 0.0001$), Interaction ($F_{(5,65)} = 0.08296$, $p = 0.9947$). ***P***, Two-way repeated-measures ANOVA: *Nox1* KD ($F_{(1,13)} < 0.001$, $p > 0.9999$), Session number ($F_{(7,91)} = 7.467$, $p < 0.0001$), Interaction ($F_{(7,91)} = 0.3760$, $p = 0.9141$). ***Q***, Two-way repeated-measures ANOVA: *Nox1* KD ($F_{(1,13)} = 12.46$, $p = 0.0037$), Session number ($F_{(4,52)} = 12.46$, $p < 0.0001$), Interaction ($F_{(4,52)} = 2.834$, $p = 0.0335$). Bonferroni post-test: $^{*}p < 0.05$; $^{**}p < 0.01$. Lines with and without symbols indicate mean values and individual data points, respectively.

Consistently, OCD patients show increased functional connectivity between the OFC and striatum (Harrison et al., 2009; Dong et al., 2019), suggesting a correlation between compulsive repetitive behavior and abnormal activity in the associative striatum. Herein, we demonstrated that, in the CS, which is classified as a part of the associative striatum (Chuhma et al., 2017), repeated stimulation of D_2 receptors facilitated excitatory inputs to iMSNs in a NOX1-dependent manner. Additionally, the upregulation of *Nox1* mRNA and accumulation of activated Src in response to repeated stimulation of D_2 receptors were predominantly

observed in the CS, supporting the idea that the repetitive chewing behavior induced by QNP sensitization reflects compulsivity rather than involuntary movements, such as dyskinesia. In this context, the NOX1-mediated modulation of the CS may be one of the pathogenic mechanisms of compulsive behavioral repetition.

Nox1 deficiency improved QNP sensitization-induced reversal learning deficits, as well as repetitive behavior. As widely reported, the striatum is involved in flexible decision-making (Macpherson et al., 2014). Lesions of the dorsomedial striatum, a part of the associative striatum, increase perseverative errors during the reversal learning task, whereas lesions of dorsolateral striatum, classified as the motor striatum, do not affect reversal learning (Castañé et al., 2010). In addition, chemogenetic inhibition of striatal iMSNs disrupts reversal learning (Kwak and Jung, 2019). These observations support the idea that NOX1-mediated modulation of the CS iMSNs is responsible for perseveration during reversal learning in sensitized mice.

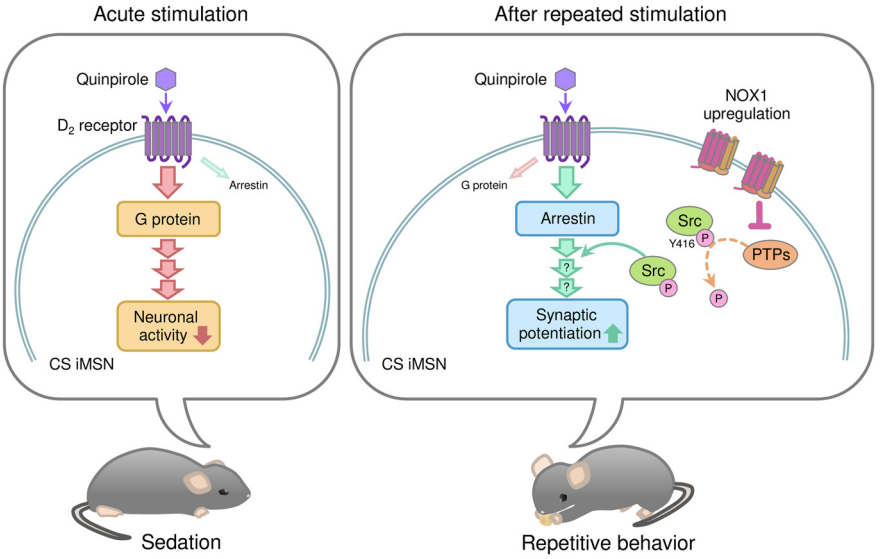

Figure 11. A hypothetical mechanism for the induction of repetitive behavior in QNP-sensitized mice. The acute stimulation of D_2 receptors induces sedation mainly through the G-protein-mediated pathway. After repeated stimulation of D_2 receptors, NOX1 expression was upregulated in the CS. In QNP-sensitized mice, no apparent repetitive behavior, Src activation, and synaptic facilitation were observed before stimulation of D_2 receptors. In contrast, once QNP was injected, activated Src accumulated in a NOX1-dependent manner. Under this condition, β-arrestin-mediated D_2 receptor signaling was increased, resulting in the facilitation of excitatory inputs in CS iMSNs. Such signal modification shifted the behavioral response from sedation to repetitive behavior.

Our observation of CS-specific upregulation of *Nox1* mRNA induced by repeated D_2 receptor stimulation suggested a heterogeneous response to D_2 receptor stimulation between striatal subregions. In support of this, various regional differences in the striatum have been reported, including gene expression patterns (Puighermanal et al., 2020), the proportion of iMSNs (Gangarossa et al., 2013), and distribution of heteromeric D_2 receptors (A_{2A}-D_2 receptor: He et al., 2016; D_1-D_2 receptor: Hasbi et al., 2020). Additionally, recent evidence indicates the difference in D_2 receptor signaling in iMSNs between dorsal and ventral striatum (Marcott et al., 2018). Although the precise regulatory mechanisms for *Nox1* expression remain to be elucidated, such regional differences in dopaminergic signaling may be involved in the local upregulation of *Nox1* mRNA.

The present electrophysiological recordings suggest the significant involvement of NOX1-derived ROS in the facilitation of excitatory inputs in striatal iMSNs. The ROS-mediated modulation of glutamatergic input has long been recognized (Thiels et al., 2000); however, the modulation pattern is unlikely to be unidirectional. For example, NOX2-derived ROS is required for both electrically induced synaptic potentiation and depression in cortical neurons (De Pasquale et al., 2014). Additionally, consistent with the present results, the removal of ROS did not affect basal synaptic transmission (Thiels et al., 2000). These findings suggest that ROS modulate synaptic transmission in response to other initiation stimuli, such as high-frequency stimulation and receptor activation. In this context, NOX1 may contribute to various forms of synaptic modulation in the striatum other than that observed in the present study. While future studies are needed, the present results suggest that NOX1 functions as a key modulator of synaptic transmission in the striatum.

Both mRNA expression and electrophysiological recording were performed >12 h after the last injection of QNP, when mice rarely showed any chewing behavior (Asaoka et al., 2019). Although upregulation of *Nox1* mRNA in the CS of sensitized mice was observed under this condition, there was no significant change in baseline excitatory inputs in the CS iMSN of sensitized mice. These observations suggest that, in addition to NOX1-derived ROS, agonist-induced recruitment of β-arrestin to D_2 receptors in the CS was also required for synaptic facilitation in iMSNs and behavioral repetition in sensitized mice. A growing body of evidence indicates that β-arrestin recruitment initiates not only receptor internalization, but also intracellular signaling (Pierce and Lefkowitz, 2001). β-arrestin-mediated signaling contributes to various neuronal functions, including synaptic plasticity in the hippocampus (Eng et al., 2016) and locomotor response to amphetamine (Beaulieu et al., 2005). Since we have previously reported that local infusion of a D_2 receptor antagonist into the CS suppressed behavioral repetition in sensitized mice (Asaoka et al., 2019), it is conceivable that β-arrestin-mediated initiation of intracellular signaling, rather than reduction in G-protein-mediated signaling, may contribute to synaptic and behavioral abnormalities in sensitized mice.

In both *in vivo* and *in vitro* experiments, NOX1-mediated inhibition of PTP activity was observed in the drug-naive condition, suggesting constitutive inhibition of PTP via NOX1-derived ROS. Supporting this idea, the activity control of nonphagocytic NOX1 is relatively lenient compared with that of NOX2. Because of the autoinhibitory region in the auxiliary subunit, p47phox, NOX2-mediated ROS production is strictly regulated (Lambeth, 2004), resulting in the phasic production of ROS, such as the "oxidative burst" in phagocytes. In contrast, because of the lack of the autoinhibitory region in NOXO1, the auxiliary subunit of NOX1 (Cheng and Lambeth, 2004) NOX1 produces ROS without any stimulation (Cheng and Lambeth, 2004). Therefore, in combination with the high expression of *Nox1* mRNA in the striatum, the constitutive activity of NOX1 may be responsible for the tonic inhibition of PTP activity in the striatum.

In parallel with the CS-specific upregulation of *Nox1* mRNA, accumulation of activated Src was observed in the CS of sensitized mice; however, NOX1-mediated PTP inhibition alone appeared to be insufficient for the accumulation of activated Src.

Since the amino acid sequence responsible for ROS-mediated inhibition is highly conserved in PTP subtypes (Lohse et al., 1997), ROS broadly inhibit PTPs (Meng et al., 2002), potentially resulting in the global stabilization of phosphorylated tyrosine residues. Considering that the activity of Src is oppositely regulated by the phosphorylation of two distinct tyrosine residues, Y416 and Y527 (Zheng et al., 1992), the NOX1-mediated inhibition of PTPs may contribute to the stabilization of both the active and inactive forms of Src, rather than the selective accumulation of the active form. Therefore, the accumulation of activated Src in sensitized mice may be observed as a result of the synergistic combination of NOX1-mediated inhibition of PTPs and β-arrestin-mediated positive allosteric modulation of the autophosphorylation of Src at Y416 (Yang et al., 2018); however, further studies are warranted.

Recruitment of β-arrestin to D_2 receptors subsequently induces receptor internalization as well as initiation of intracellular signaling. Clinical imaging studies revealed a reduction in D_2 receptor binding availability, which reflects low membrane expression of D_2 receptor and/or increased dopamine release, in the striatum of patients with OCD and substance use disorder (Denys et al., 2004; Fehr et al., 2008; Lee et al., 2009). Similar observations have also been reported in animal models of OCD and addiction (Nader et al., 2006; Manning et al., 2020). These observations raise the possibility that β-arrestin-mediated D_2 receptor internalization is facilitated in patients with compulsivity, supporting the present observation in QNP-sensitized mice.

In conclusion, we herein demonstrated the contribution of striatal region-specific upregulation of *Nox1* expression to behavioral repetition induced by repeated D_2 receptor stimulation. β-arrestin recruitment and subsequent intracellular signaling, represented by Src activation, were required and sufficient for synaptic facilitation in iMSNs, whereas repetitive behavior, perseverative behavior, and synaptic abnormalities were attenuated by genetic deletion or pharmacological inhibition of NOX1. Since abnormal D_2 receptor signaling is widely suggested in patients with compulsivity, the present results indicate that NOX1 has potential as a druggable target for the treatment of compulsivity represented by behavioral repetition.

References

Ahmari SE, Spellman T, Douglass NL, Kheirbek MA, Simpson HB, Deisseroth K, Gordon JA, Hen R (2013) Repeated cortico-striatal stimulation generates persistent OCD-like behavior. Science 340:1234–1239.

Arakawa N, Katsuyama M, Matsuno K, Urao N, Tabuchi Y, Okigaki M, Matsubara H, Yabe-Nishimura C (2006) Novel transcripts of Nox1 are regulated by alternative promoters and expressed under phenotypic modulation of vascular smooth muscle cells. Biochem J 398:303–310.

Asaoka N, Nagayasu K, Nishitani N, Yamashiro M, Shirakawa H, Nakagawa T, Kaneko S (2015) Inhibition of histone deacetylases enhances the function of serotoninergic neurons in organotypic raphe slice cultures. Neurosci Lett 593:72–77.

Asaoka N, Nishitani N, Kinoshita H, Nagai Y, Hatakama H, Nagayasu K, Shirakawa H, Nakagawa T, Kaneko S (2019) An adenosine A_{2A} receptor antagonist improves multiple symptoms of repeated quinpirole-induced psychosis. eNeuro 6:72ENEURO.0366-18.2019.

Bailey A, Metaxas A, Yoo JH, McGee T, Kitchen I (2008) Decrease of D_2 receptor binding but increase in D_2-stimulated G-protein activation, dopamine transporter binding and behavioural sensitization in brains of mice treated with a chronic escalating dose 'binge' cocaine administration paradigm. Eur J Neurosci 28:759–770.

Bariselli S, Fobbs WC, Creed MC, Kravitz AV (2019) A competitive model for striatal action selection. Brain Res 1713:70–79.

Baxter LR Jr, Phelps ME, Mazziotta JC, Guze BH, Schwartz JM, Selin CE (1987) Local cerebral glucose metabolic rates in obsessive-compulsive disorder: a comparison with rates in unipolar depression and in normal controls. Arch Gen Psychiatry 44:211–218.

Beaulieu JM, Sotnikova TD, Marion S, Lefkowitz RJ, Gainetdinov RR, Caron MG (2005) An Akt/beta-arrestin 2/PP2A signaling complex mediates dopaminergic neurotransmission and behavior. Cell 122:261–273.

Bloch MH, Landeros-Weisenberger A, Kelmendi B, Coric V, Bracken MB, Leckman JF (2006) A systematic review: antipsychotic augmentation with treatment refractory obsessive-compulsive disorder. Mol Psychiatry 11:622–632.

Bock R, Shin JH, Kaplan AR, Dobi A, Markey E, Kramer PF, Gremel CM, Christensen CH, Adrover MF, Alvarez VA (2013) Strengthening the accumbal indirect pathway promotes resilience to compulsive cocaine use. Nat Neurosci 16:632–638.

Calabresi P, Picconi B, Tozzi A, Ghiglieri V, Di Filippo M (2014) Direct and indirect pathways of basal ganglia: a critical reappraisal. Nat Neurosci 17:1022–1030.

Castañé A, Theobald DE, Robbins TW (2010) Selective lesions of the dorsomedial striatum impair serial spatial reversal learning in rats. Behav Brain Res 210:74–83.

Cheng G, Lambeth JD (2004) NOXO1, regulation of lipid binding, localization, and activation of Nox1 by the Phox homology (PX) domain. J Biol Chem 279:4737–4742.

Chuhma N, Mingote S, Kalmbach A, Yetnikoff L, Rayport S (2017) Heterogeneity in dopamine neuron synaptic actions across the striatum and its relevance for schizophrenia. Biol Psychiatry 81:43–51.

De Pasquale R, Beckhauser TF, Hernandes MS, Giorgetti Britto LR (2014) LTP and LTD in the visual cortex require the activation of NOX2. J Neurosci 34:12778–12787.

Denys D, van der Wee N, Janssen J, De Geus F, Westenberg HG (2004) Low level of dopaminergic D2 receptor binding in obsessive-compulsive disorder. Biol Psychiatry 55:1041–1045.

Dong C, Yang Q, Liang J, Seger CA, Han H, Ning Y, Chen Q, Peng Z (2019) Impairment in the goal-directed corticostriatal learning system as a biomarker for obsessive-compulsive disorder. Psychol Med 5:1490–1500.

Eng AG, Kelver DA, Hedrick TP, Swanson GT (2016) Transduction of group I mGluR-mediated synaptic plasticity by β-arrestin2 signalling. Nat Commun 7:13571.

Farkas S, Nagy K, Jia Z, Hortobágyi T, Varrone A, Halldin C, Csiba L, Gulyás B (2012) Signal transduction pathway activity compensates dopamine D_2/D_3 receptor density changes in Parkinson's disease: a preliminary comparative human brain receptor autoradiography study With [^{3}H] raclopride and [^{35}S]GTPγS. Brain Res 1453:56–63.

Fasano A, Petrovic I (2010) Insights into pathophysiology of punding reveal possible treatment strategies. Mol Psychiatry 15:560–573.

Fehr C, Yakushev I, Hohmann N, Buchholz HG, Landvogt C, Deckers H, Eberhardt A, Kläger M, Smolka MN, Scheurich A, Dielentheis T, Schmidt LG, Rösch F, Bartenstein P, Gründer G, Schreckenberger M (2008) Association of low striatal dopamine D2 receptor availability with nicotine dependence similar to that seen with other drugs of abuse. Am J Psychiatry 165:507–514.

Fieblinger T, Graves SM, Sebel LE, Alcacer C, Plotkin JL, Gertler TS, Chan CS, Heiman M, Greengard P, Cenci MA, Surmeier DJ (2014) Cell type-specific plasticity of striatal projection neurons in parkinsonism and L-DOPA-induced dyskinesia. Nat Commun 5:5316.

Franklin BJ, Paxinos G (2007) The mouse brain in stereotaxic coordinates, Ed 3. San Diego: Academic.

Gangarossa G, Espallergues J, Mailly P, De Bundel D, de Kerchove d'Exaerde A, Hervé D, Girault JA, Valjent E, Krieger P (2013) Spatial distribution of D1R- and D2R-expressing medium-sized spiny neurons differs along the rostro-caudal axis of the mouse dorsal striatum. Front Neural Circuits 7:124.

Graybiel AM, Rauch SL (2000) Toward a neurobiology of obsessive-compulsive disorder. Neuron 28:343–347.

Harrison BJ, Soriano-Mas C, Pujol J, Ortiz H, López-Solà M, Hernández-Ribas R, Deus J, Alonso P, Yücel M, Pantelis C, Menchon JM, Cardoner N (2009) Altered corticostriatal functional connectivity in obsessive-compulsive disorder. Arch Gen Psychiatry 66:1189–1200.

Hasbi A, Madras BK, Bergman J, Kohut S, Lin Z, Withey SL, George SR (2020) Δ-Tetrahydrocannabinol increases dopamine D1-D2 receptor heteromer and elicits phenotypic reprogramming in adult primate striatal neurons. iScience 23:100794.

He Y, Li Y, Chen M, Pu Z, Zhang F, Chen L, Ruan Y, Pan X, He C, Chen X, Li Z, Chen JF (2016) Habit formation after random interval training is associated with increased adenosine A2A receptor and dopamine D2 receptor heterodimers in the striatum. Front Mol Neurosci 9:151.

Holmström KM, Finkel T (2014) Cellular mechanisms and physiological consequences of redox-dependent signalling. Nat Rev Mol Cell Biol 15:411–421.

Hu Y, Salmeron BJ, Krasnova IN, Gu H, Lu H, Bonci A, Cadet JL, Stein EA, Yang Y (2019) Compulsive drug use is associated with imbalance of orbitofrontal- and prelimbic-striatal circuits in punishment-resistant individuals. Proc Natl Acad Sci USA 116:9066–9071.

Huang L, Wu DD, Zhang L, Feng LY (2013) Modulation of A2a receptor antagonist on D2 receptor internalization and ERK phosphorylation. Acta Pharmacol Sin 34:1292–1300.

Hyman SE, Malenka RC (2001) Addiction and the brain: the neurobiology of compulsion and its persistence. Nat Rev Neurosci 2:695–703.

Ibi M, Matsuno K, Shiba D, Katsuyama M, Iwata K, Kakehi T, Nakagawa T, Sango K, Shirai Y, Yokoyama T, Kaneko S, Saito N, Yabe-Nishimura C (2008) Reactive oxygen species derived from NOX1/NADPH oxidase enhance inflammatory pain. J Neurosci 28:9486–9494.

Ibi M, Matsuno K, Matsumoto M, Sasaki M, Nakagawa T, Katsuyama M, Iwata K, Zhang J, Kaneko S, Yabe-Nishimura C (2011) Depressive-like behaviors are regulated by NOX1/NADPH oxidase by redox modification of NMDA receptor 1. J Neurosci 31:18094–18103.

Kroeze WK, Sassano MF, Huang XP, Lansu K, McCorvy JD, Giguère PM, Sciaky N, Roth BL (2015) PRESTO-Tango as an open-source resource for interrogation of the druggable human GPCRome. Nat Struct Mol Biol 22:362–369.

Kwak S, Jung MW (2019) Distinct roles of striatal direct and indirect pathways in value-based decision making. Elife 8:e46050.

Lambeth JD (2004) NOX enzymes and the biology of reactive oxygen. Nat Rev Immunol 4:181–189.

Lee B, London ED, Poldrack RA, Farahi J, Nacca A, Monterosso JR, Mumford JA, Bokarius AV, Dahlbom M, Mukherjee J, Bilder RM, Brody AL, Mandelkern MA (2009) Striatal dopamine D_2/D_3 receptor availability is reduced in methamphetamine dependence and is linked to impulsivity. J Neurosci 29:14734–14740.

Li YC, Kellendonk C, Simpson EH, Kandel ER, Gao WJ (2011) D_2 receptor overexpression in the striatum leads to a deficit in inhibitory transmission and dopamine sensitivity in mouse prefrontal cortex. Proc Natl Acad Sci USA 108:12107–12112.

Lohse DL, Denu JM, Santoro N, Dixon JE (1997) Roles of aspartic acid-181 and serine-222 in intermediate formation and hydrolysis of the mammalian protein-tyrosine-phosphatase PTP1. Biochemistry 36:4568–4575.

Loonen AJ, Ivanova SA (2013) New insights into the mechanism of drug-induced dyskinesia. CNS Spectr 18:15–20.

Lorenz U (2011) Protein tyrosine phosphatase assays. Curr Protoc Immunol Chapter 11:Unit 11.7.

Luttrell LM, Lefkowitz RJ (2002) The role of beta-arrestins in the termination and transduction of G-protein-coupled receptor signals. J Cell Sci 115:455–465.

MacDonald BC, Davey GC (2005) A mood-as-input account of perseverative checking: the relationship between stop rules, mood and confidence in having checked successfully. Behav Res Ther 43:69–91.

Macpherson T, Morita M, Hikida T (2014) Striatal direct and indirect pathways control decision-making behavior. Front Psychol 5:1301.

Manning EE, Wang AY, Saikali LM, Winner AS, Ahmari SE (2020) Disruption of prepulse inhibition is associated with severity of compulsive behavior and nucleus accumbens dopamine receptor changes in Sapap3 knockout mice. bioRxiv 694935.

Marcott PF, Gong S, Donthamsetti P, Grinnell SG, Nelson MN, Newman AH, Birnbaumer L, Martemyanov KA, Javitch JA, Ford CP (2018) Regional heterogeneity of D2-receptor signaling in the dorsal striatum and nucleus accumbens. Neuron 98:575–587.

Matsuno K, Yamada H, Iwata K, Jin D, Katsuyama M, Matsuki M, Takai S, Yamanishi K, Miyazaki M, Matsubara H, Yabe-Nishimura C (2005) Nox1 is involved in angiotensin II-mediated hypertension: a study in Nox1-deficient mice. Circulation 112:2677–2685.

McClung CA, Nestler EJ (2003) Regulation of gene expression and cocaine reward by CREB and DeltaFosB. Nat Neurosci 6:1208–1215.

Meng TC, Fukada T, Tonks NK (2002) Reversible oxidation and inactivation of protein tyrosine phosphatases in vivo. Mol Cell 9:387–399.

Moreno-López L, Perales JC, van Son D, Albein-Urios N, Soriano-Mas C, Martinez-Gonzalez JM, Wiers RW, Verdejo-García A (2015) Cocaine use severity and cerebellar gray matter are associated with reversal learning deficits in cocaine-dependent individuals. Addict Biol 20:546–556.

Nader MA, Morgan D, Gage HD, Nader SH, Calhoun TL, Buchheimer N, Ehrenkaufer R, Mach RH (2006) PET imaging of dopamine D_2 receptors during chronic cocaine self-administration in monkeys. Nat Neurosci 9:1050–1056.

Pierce KL, Lefkowitz RJ (2001) Classical and new roles of beta-arrestins in the regulation of G-protein-coupled receptors. Nat Rev Neurosci 2:727–733.

Puighermanal E, Castell L, Esteve-Codina A, Melser S, Kaganovsky K, Zussy C, Boubaker-Vitre J, Gut M, Rialle S, Kellendonk C, Sanz E, Quintana A, Marsicano G, Martin M, Rubinstein M, Girault JA, Ding JB, Valjent E (2020) Functional and molecular heterogeneity of D2R neurons along dorsal ventral axis in the striatum. Nat Commun 11:1957.

Robbins TW, Vaghi MM, Banca P (2019) Obsessive-compulsive disorder: puzzles and prospects. Neuron 102:27–47.

Shen W, Flajolet M, Greengard P, Surmeier DJ (2008) Dichotomous dopaminergic control of striatal synaptic plasticity. Science 321:848–851.

Sorce S, Krause KH, Jaquet V (2012) Targeting NOX enzymes in the central nervous system: therapeutic opportunities. Cell Mol Life Sci 69:2387–2407.

Szechtman H, Sulis W, Eilam D (1998) Quinpirole induces compulsive checking behavior in rats: a potential animal model of obsessive-compulsive disorder (OCD). Behav Neurosci 112:1475–1485.

Tezcan D, Tumkaya S, Bora E (2017) Reversal learning in patients with obsessive-compulsive disorder (OCD) and their unaffected relatives: is orbitofrontal dysfunction an endophenotype of OCD? Psychiatry Res 252:231–233.

Thiels E, Urban NN, Urban NN, Gonzalez-Burgos GR, Kanterewicz BI, Barrionuevo G, Chu CT, Oury TD, Klann E (2000) Impairment of long-term potentiation and associative memory in mice that overexpress extracellular superoxide dismutase. J Neurosci 20:7631–7639.

Tokunaga N, Choudhury ME, Nishikawa N, Nagai M, Tujii T, Iwaki H, Kaneta M, Nomoto M (2012) Pramipexole upregulates dopamine receptor D_2 and D_3 expression in rat striatum. J Pharmacol Sci 120:133–137.

Tritsch NX, Sabatini BL (2012) Dopaminergic modulation of synaptic transmission in cortex and striatum. Neuron 76:33–50.

Vanderschuren LJ, Everitt BJ (2004) Drug seeking becomes compulsive after prolonged cocaine self-administration. Science 305:1017–1019.

Voon V, Fernagut PO, Wickens J, Baunez C, Rodriguez M, Pavon N, Juncos JL, Obeso JA, Bezard E (2009) Chronic dopaminergic stimulation in Parkinson's disease: from dyskinesias to impulse control disorders. Lancet Neurol 8:1140–1149.

Wang W, Li C, Chen Q, van der Goes MS, Hawrot J, Yao AY, Gao X, Lu C, Zang Y, Zhang Q, Lyman K, Wang D, Guo B, Wu S, Gerfen CR, Fu Z, Feng G (2017) Striatopallidal dysfunction underlies repetitive behavior in Shank3-deficient model of autism. J Clin Invest 127:1978–1990.

Welch JM, Lu J, Rodriguiz RM, Trotta NC, Peca J, Ding JD, Welch JM, Lu J, Rodriguiz RM, Trotta NC, Peca J, Ding JD, Feliciano C, Chen M, Adams JP, Luo J, Dudek SM, Weinberg RJ, Calakos N, Wetsel WC, et al. (2007) Cortico-striatal synaptic defects and OCD-like behaviours in Sapap3-mutant mice. Nature 448:894–900.

Xia J, Meyers AM, Beeler JA (2017) Chronic nicotine alters corticostriatal plasticity in the striatopallidal pathway mediated by NR2B-containing silent synapses. Neuropsychopharmacology 42:2314–2324.

Yang F, Xiao P, Qu CX, Liu Q, Wang LY, Liu ZX, He QT, Liu C, Xu JY, Li RR, Li MJ, Li Q, Guo XZ, Yang ZY, He DF, Yi F, Ruan K, Shen YM, Yu X, Sun JP, et al. (2018) Allosteric mechanisms underlie GPCR signaling to SH3-domain proteins through arrestin. Nat Chem Biol 14:876–886.

Zhang D, Zhang L, Tang Y, Zhang Q, Lou D, Sharp FR, Zhang J, Xu M (2005) Repeated cocaine administration induces gene expression changes through the dopamine D_1 receptors. Neuropsychopharmacology 30:1443–1454.

Zheng XM, Wang Y, Pallen CJ (1992) Cell transformation and activation of pp60c-src by overexpression of a protein tyrosine phosphatase. Nature 359:336–339.